NASA TECHNICAL NOTE

NASA TN D-7008

IMP I OPTICAL ASPECT SYSTEM

by E. John Pyle

Goddard Space Flight Center
Greenbelt, Md. 20771

NATIONAL AERONAUTICS AND SPACE ADMINISTRATION • WASHINGTON, D. C. • MARCH 1971

1. Report No.	2. Government Accession No.	3. Recipient's Catalog No.
NASA TN D-7008		

4. Title and Subtitle

IMP I Optical Aspect System

5. Report Date: March 1971

6. Performing Organization Code

7. Author(s): E. John Pyle

8. Performing Organization Report No.: G-993

9. Performing Organization Name and Address

Goddard Space Flight Center
Greenbelt, Maryland 20771

10. Work Unit No.

11. Contract or Grant No.

13. Type of Report and Period Covered: Technical Note

12. Sponsoring Agency Name and Address

National Aeronautics and Space Administration
Washington, D.C. 20546

14. Sponsoring Agency Code

15. Supplementary Notes

16. Abstract

Two detectors are used to obtain information from the sun and the sunlit earth. A digital solar sensor that performs an optical analog-to-digital conversion is used to measure the elevation and azimuth angles of the solar disk. Information on the sunlit earth is obtained by the use of a visible-horizon detector. The logic system necessary to collect, process, and store information from these two detectors is presented and discussed.

Sun-line crossing, detected by the solar sensor, is used to generate an onboard clock signal synchronized to the spacecraft rotation rate. The Spin Synchronous Clock, which divides the spin period into 128 intervals, is also presented and discussed.

17. Key Words Suggested by Author	18. Distribution Statement
Attitude Determination Optical Sensing IMP I	Unclassified—Unlimited

19. Security Classif. (of this report)	20. Security Classif. (of this page)	21. No. of Pages	22. Price*
Unclassified	Unclassified	64	$3.00

*For sale by the National Technical Information Service, Springfield, Virginia 22151

CONTENTS

IMP I OPTICAL ASPECT SYSTEM

by
E. John Pyle
Goddard Space Flight Center

INTRODUCTION

The problem of attitude or aspect determination is the problem of defining the angular relationship between two coordinate systems, one fixed in a reference space and the other fixed in the spacecraft. There are six degrees of freedom associated with a general coordinate system, with respect to a reference coordinate system. Three of these concern the translational motion of the center of mass of the spacecraft, which is a problem in orbit and trajectory calculations. The remaining three degrees of freedom deal with the rotational motion of the spacecraft about its center of mass. The measurement of this rotational motion is called "aspect determination."

A body spinning in free space has most of the properties of a gyroscope; if a spin is imparted to a spacecraft at the time of injection into orbit, it performs like a gyroscope while traveling in free space. An aspect system included in the spacecraft assembly gives the orientation of the spacecraft's spin axis. Since there are three degrees of rotational freedom of a rigid body associated with aspect determination, the instrumentation in the aspect system must be capable of measuring at least three parameters.

This paper discusses the IMP I Aspect System; Figure 1 is an overall block diagram. The parameters measured are the elevation angles—with respect to the spin axis—of the sun, β, and the earth, δ; the order of observation; and the fraction of one spin period between the observation of each. Additional information such as the position of the spacecraft with respect to the two observed references is required; this is available from earth-based observations.

The order of observation and the fraction of a spin period between observations can be measured on board the spacecraft. These may be derived from a knowledge of the exact times that a specified reference plane crosses the solar and terrestrial disks. These times must be related to some known time standard; these relationships must be remembered, encoded, and presented to the transmitter. Two sensors will be used to determine the angle between the spin axis of the vehicle and each of the two references. Since the sun, for practical purposes, is a point source to the sun sensor, the vector from the spacecraft to the sun is an axis of symmetry. This means that the locus of the spin axis is a cone whose axis is the sun vector and whose half-angle β is the angle measured by the sun sensor, that is, the angle between the spin axis and the sun vector. In order to calculate the position of the spacecraft's spin axis, a measurement must be made with regard to another reference—the earth. The aspect system

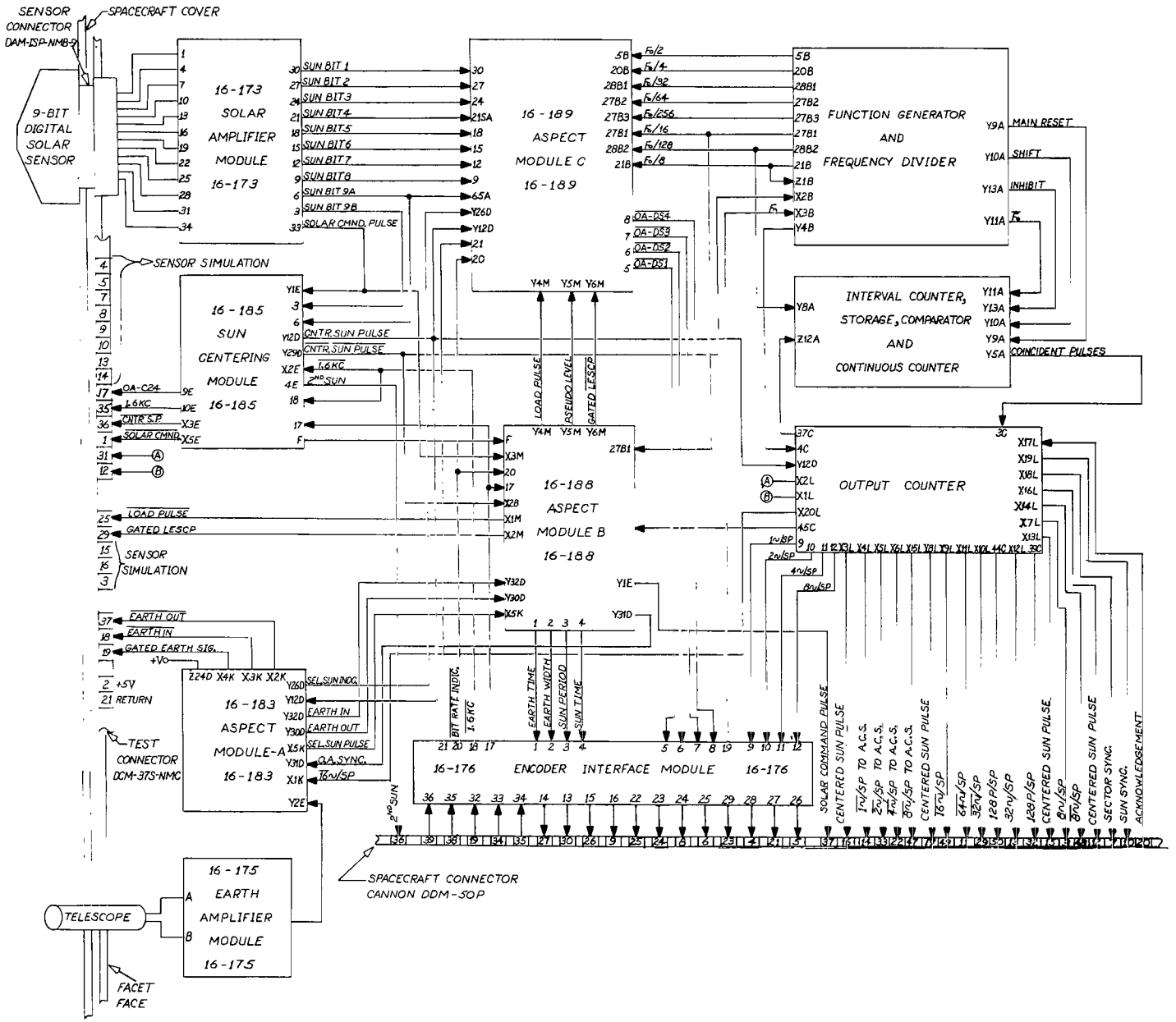

Figure 1—System block diagram.

therefore will contain an earth sensor, sensitive to visible light, with a narrow field of view mounted so as to scan 90 degrees from the spin axis. Information from this sensor will lead to the calculation of the angle between the spacecraft spin axis and the vector from the center of the earth through the center of gravity of the spacecraft. This vector, also, is an axis of symmetry, and the locus of the spin axis is a cone whose axis is this earth-spacecraft vector and whose half-angle δ is the angle calculated from earth-sensor information. Hence the spin axis must be at one of the points of intersection of the two cones (see Figure 2). An unambiguous solution is obtained when the two other parameters measured on board the spacecraft are taken into account.

The Spin Synchronous Clock (SSC) is a digital system that generates a time-based clock signal synchronized to the spin rate of the spin-stabilized spacecraft. The basic function of the device is to generate 2^n (where $n = 7$) pulses per spin period. These pulses divide the spin period into $2^n - 1$ equal time intervals plus one remaining interval, which may be slightly greater or smaller than the other intervals. To accomplish this function the SSC receives a high-frequency signal $f_0 = 25.6$ kHz from the

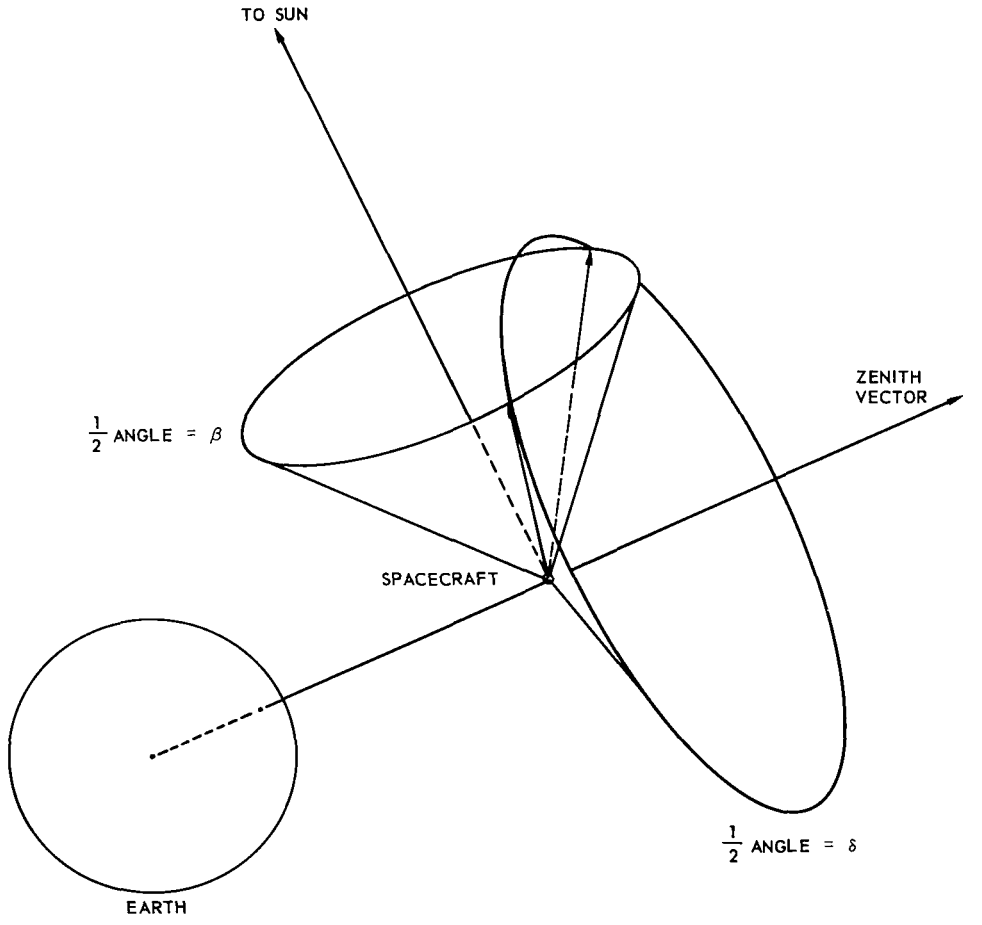

Figure 2—Relationship between the spacecraft spin axis and the intersection of the two locus cones.

spacecraft encoder. The command pulse defining the rotational period is generated in the optical-aspect electronics and fed to the SSC.

ASPECT SENSORS

The energy emanating from a celestial body can be detected by sensitive measuring instruments. The optics, fields of view, and other characteristic parameters of these sensors are predicated on the energy source selected and the particular sensor application.

Attitude can be derived from the spin-axis orientation relative to any number of celestial objects. A minimum of two objects (sun and earth) is necessary to completely specify the spin-axis attitude of the spacecraft. The sun can be treated as a point source, whereas the earth's angular subtense varies as a function of relative sun position and closeness of the detecting instrument.

Digital Solar Sensor

The digital solar sensor (Figure 3) measures the angle of incident sunlight with respect to the sensor Z-axis and expresses this angle as a digital number. The incident sunlight, passing through a slit on the top of a quartz block, is screened by a gray-coded pattern on the bottom of the block to illuminate or not illuminate each of the photocell detectors. The angle of incidence determines which combination of photocells is illuminated. The solar sensor also includes a command slit, which is mounted perpendicular to the gray-coded reticle. If the sensor is rotated about a vertical axis along the command slit, the field of view of the two slits will sweep over a solid angle. When the plane containing the command slit passes across the solar disk, one or more of the photocells will be illuminated. The time that this illumination occurs provides a measurement of the azimuth angle of the sun. The particular combination of photocells that is illuminated provides a digital measurement of the elevation angle of the sun in sensor coordinates.

The digital solar sensor has features that make it more desirable than the analog types of solar sensors: (1) It is not subject to errors introduced by earth shine, (2) there are no components that can drift, (3) no in-flight calibration is required, (4) the weight is small, and (5) power is needed only to drive the output load.

Earth-Horizon Detector

The horizon detector consists of a simple telescope and lens. The detector element is a photodiode, which is placed at the focal point of the lens. The field of view of the horizon detector is a pencil beam approximately 1 degree in diameter. If the detector is mounted at an angle, γ, from the spin axis of a rotating spacecraft, the field of view of the detector will traverse the surface of a cone whose half angle is equal to γ. When the field of view scans the discontinuity caused by the sunlit earth against the dark background of interplanetary space, this detector generates an output signal. This signal, after amplification, is differentiated to form pulses at its leading and trailing edges. The information contained in the relative position of these pulses to the command slit's crossing of the sun provides a measure of the inclination of the spacecraft zenith vector to the spin axis.

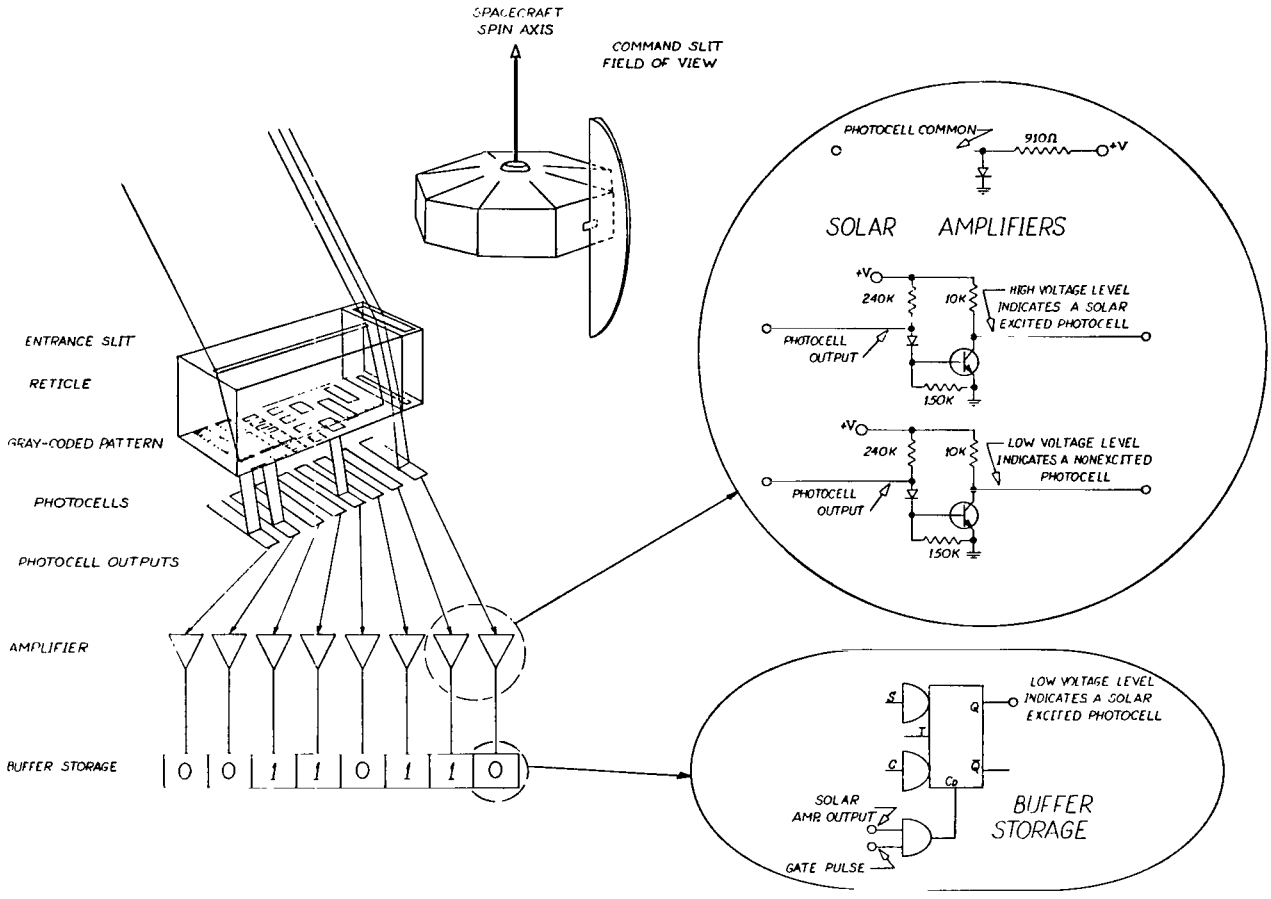

Figure 3—Schematic representation of a digital solar sensor.

ASPECT-SYSTEM ELECTRONICS

Solar-Sensor Electronics

The solar-sensor output consists of 10 channels of sun information. Nine of these contain angular information; the 10th contains time-occurrence or azimuth information.

Amplification of the output signals of the nine angular information channels produces a positive voltage when the channel is excited, i.e., when sunlight is incident on the detector (see Figure 4). These amplified signals are then placed in storage and, at the proper time, shifted through an inverter to the spacecraft encoder.

The amplified azimuth information, referred to as the "solar command pulse," occurs when the sun is in the field of view of the sensor command slit. The width of this pulse is a function of the spin rate and the command-slit field of view. This is undersirable; to eliminate these effects on pulse width, a centered sun pulse is generated at the midpoint of the solar command pulse (sun-centering module).

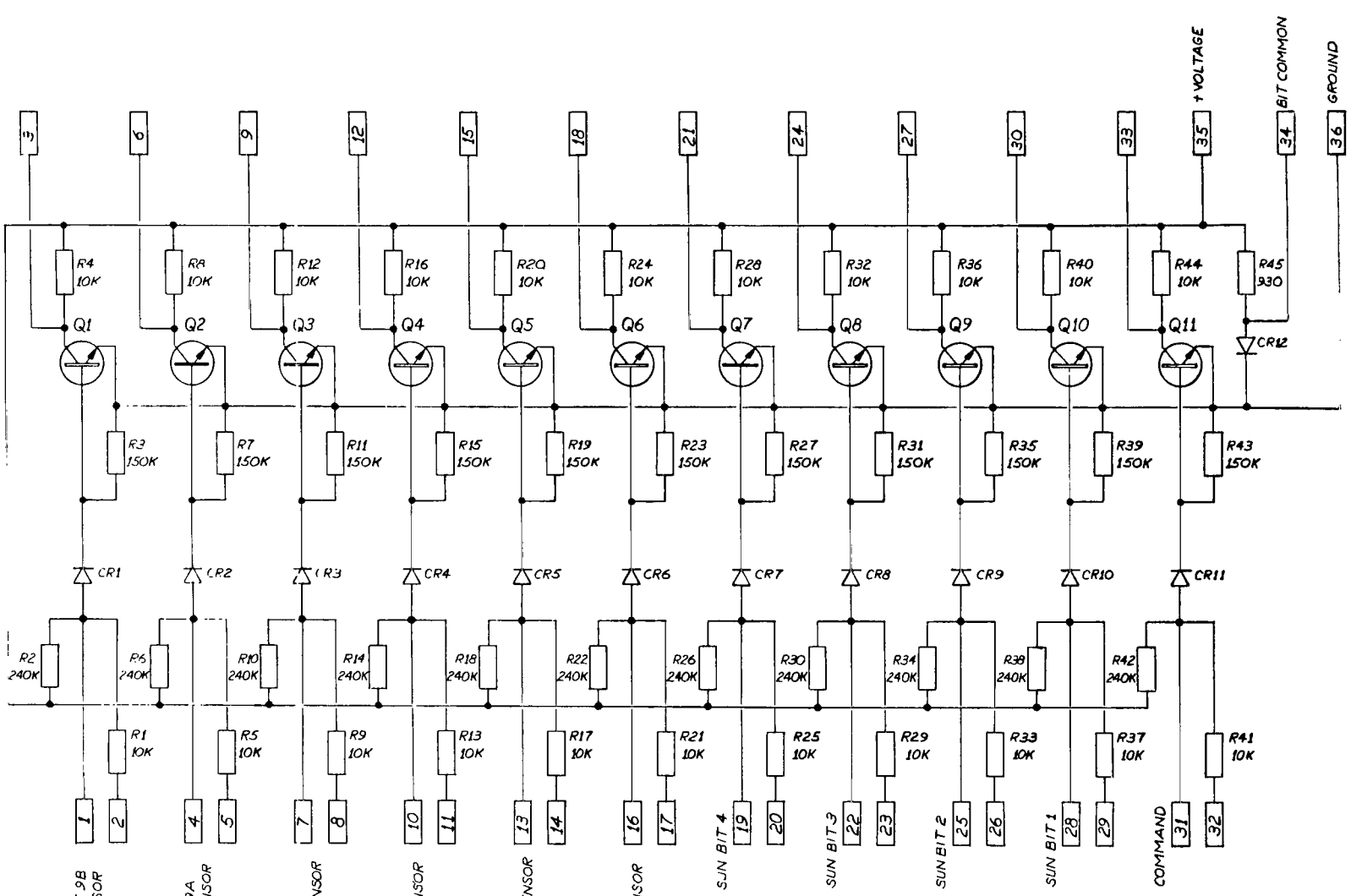

Figure 4—Solar amplifier module 16-173.

The logic that generates the centered sun pulse also produces the transfer (load) pulse, which stores the sensor's angular information (aspect module C).

The centered sun pulse is used to measure sun time and spin period. Sun time is the interval between a known spacecraft encoder function (C24) and the following centered sun pulse. Spin period is defined as the time interval between two successive centered sun pulses.

Earth-Detector Electronics

The earth detector is a light-sensing device that detects the gradient between the sunlit earth and outer space. The sensing element is a photodiode having a response that peaks at 1 micron. As the spacecraft rotates, the detector's field of view sweeps over a cone. At certain points in the orbit, the scan of this detector successively crosses the horizons and/or terminator of the sunlit earth. When this occurs, the detector produces an electrical signal. This signal is fed into a high-input-impedance amplifier, i.e., earth-amplifier module (see Figure 5). Subsequent electronic processing shapes this signal into positive pulses occurring at each intercept of the earth's horizon and/or terminator. The same processing electronics eliminates any solar information that might be caused by the earth detector's viewing the sun.

The information contained in the relative position of these earth pulses to the centered sun pulse is used to compute the spin-axis earth angle, δ. The relative position of the earth and sun pulses are contained in two measureable quantities: earth time and earth width. Earth time is defined as the interval between the centered sun pulse and the earth pulse that defines the start of an earth scan. The second interval is the time between the two earth pulses, corresponding to the apparent width of the sunlit earth.

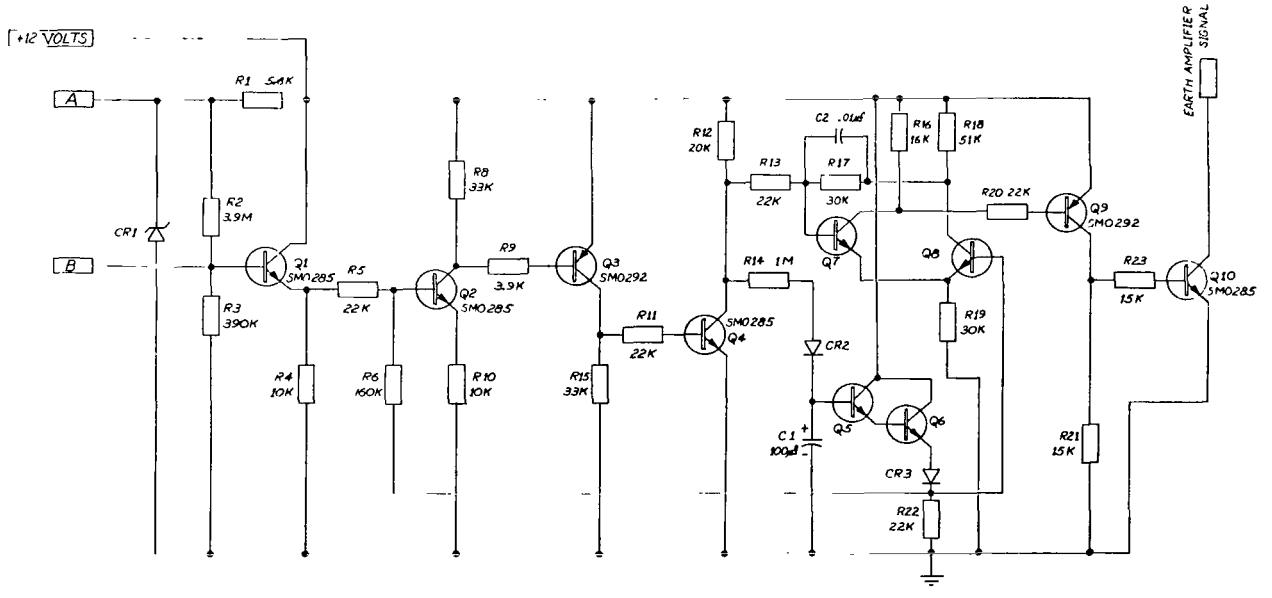

Figure 5—Earth-amplifier module 16-175.

Measurement of Aspect Parameters

The quantities measured by the aspect system are those already mentioned:

(1) Spin period.

(2) Sun time.

(3) Earth time.

(4) Earth width.

(5) Spin-axis sun angle.

As previously mentioned, the three parameters necessary for attitude determination are (1) β, the spin-axis sun angle, (2) δ, the spin-axis earth angle, and (3) the fraction of a spin period between observing each.

Spin-axis sun angle β is measured directly by the solar sensor; its digital representation is placed in storage.

Spin-axis earth angle δ must be computed from the relative position of the sun and earth (see Appendix D). This information is contained in the five quantities measured by the aspect system.

The fraction of a spin period between the observations of the two reference sources (sun and earth) can be determined from knowledge of the spin period, earth time, and earth width.

Encoder Interface

The spacecraft encoder's interface with the aspect system places certain restrictions on the measuring, processing, and storing of aspect data.

The encoder samples the aspect data once every C24 period, $T_{C24} = 81.92$ s. The encoder circuitry supplies the storage accumulators for the interval measurements, i.e., sun time, spin period, earth time, and earth width. Since the nominal spin period for the satellite is 12 s, the gates to these accumulators must be controlled so that repeated data are not fed into them; i.e., only one measurement of a particular interval time is made in 81.92 s.

To satisfy this timing restriction, the leading edge of C24 is differentiated and used as a synchronizing signal by the aspect system. The occurrence of this signal is used to initiate a series of events that provide only a single measurement of each of the above-mentioned time intervals in the 81.92-s encoder-controlled period.

The gating of the sun-time accumulator is controlled by a flipflop that is reset by the centered sun pulse and set by the aspect synchronous signal. Hence, for the time interval between the aspect synchronous signal and the first centered sun pulse, this flipflop enables the accumulator and allows a 1.6-kHz signal to be counted. Repeated occurrences of the centered sun pulse only serve to keep the flipflop in the inhibit state.

A two-stage counter, reset to zero by the aspect synchronous signal (aspect sync), controls the spin-period accumulator by generating an enable signal between the first and second centered sun pulses following reset. To prevent further generation of this enable signal during the C24 period, the input to this counter is inhibited following the second centered sun pulse. When the accumulator is enabled by its gate, a 1.6-kHz signal is used for a counting source. The trailing edge of this enable signal is also used to control the transfer pulse which sets the angular information from the solar sensor into the storage register.

The earth-time and earth-width accumulators are controlled by another two-stage counter. The first stage, which controls the earth-time accumulator, is reset by either the aspect sync or the earth's leading-edge signal. The second stage is reset by either the aspect sync or the earth's trailing-edge signal and controls the earth-width accumulator.

The action of this counter is initiated by a selected centered sun pulse. This pulse is generated once per C24 period by the first centered sun pulse following both the aspect sync signal and the earth amplifier signal. Hence, the data from the second earth scan in the C24 period is used to control the 1.6-kHz counting signal for the earth-time and earth-width accumulators.

The spin-axis sun-angle information is shifted out of its storage register once per C24 period by a series of shift pulses controlled by the encoder. The timing of these shift pulses is such that they occur well after the aspect system's generation of the transfer (load) pulse.

The above discussion was based on the encoder operation in its low bit rate mode (400 bps). The effect of the high bit rate mode (1600 bps) on the aspect data is simply to read out the same data four times in the C24 period. The added readout supplies no new data, since the C24 period generating the aspect sync signal does not change.

Figure 6 shows in detail the timing for aspect parameters.

SPIN SYNCHRONOUS CLOCK ELECTRONICS

Logic Functions

The basic function of the Spin Synchronous Clock (SSC) is to generate 2^n (where $n = 7$) pulses per spin period. These pulses divide the rotational period into $2^n - 1$ equal time intervals plus one remaining interval which may be slightly greater or smaller than the other intervals. To accomplish this function, the SSC receives a high-frequency signal f_0 of 25.6 kHz from the spacecraft encoder and uses the centered sun pulse generated by the aspect system to define the rotational period of the spacecraft.

The SSC includes the following components: a pulse generator; counters C_0, C_1, C_4, C_d, and C_t; a storage register; a comparator; and pseudo-command circuits.

Generation of the basic control functions for the SSC is provided by two counters, C_d and C_4, and associated decoding gates. These basic control functions are as follows:

(1) C_1 inhibit signal—an inhibit voltage that prevents counter C_1 from changing its contents during transfer.

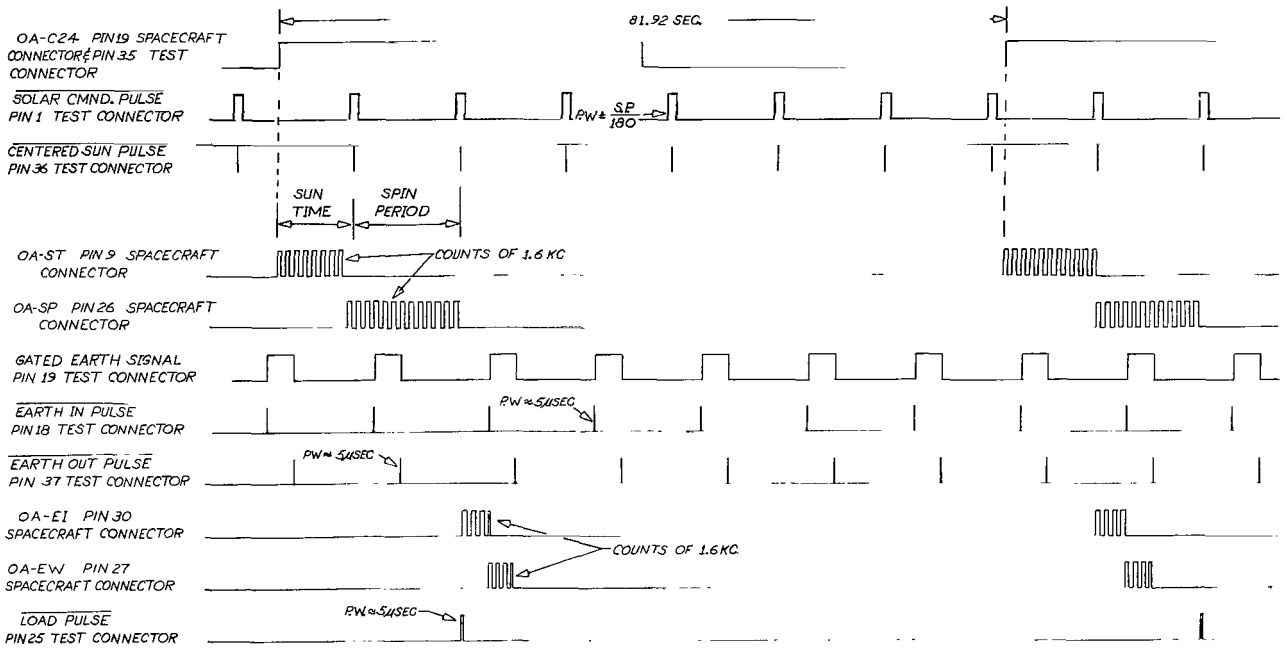

Figure 6—Aspect parameters; timing diagram.

(2) C_1 transfer pulse—a pulse that transfers the contents of counter C_1 into a storage register.

(3) C_1 reset pulse—a pulse that resets counter C_1 to zero following the transfer pulse.

The leading edge of the centered sun pulse (command pulse) resets both counters to zero, indicating the start of a rotation period. Counter C_d performs the frequency division on the f_0 signal to generate the f_1 signal ($f_1 = f_0/2^n = 25.6/128 = 0.2$ kHz = 200 Hz). The block diagram, Figure 7, shows the logic for the three basic control functions and the fact that the input to C_4 is a gated function of one of the intermediate stages of C_d. The gating insures that the basic control functions occur only once each spin period. Use of an intermediate stage of C_d as the input to C_4 merely provides reset and transfer pulses of convenient duration. The only restriction is that these control signals be completed before the first count of f_1 enters the interval counter C_1.

Upon the occurrence of the transfer pulse, the storage register accepts and retains the information from the interval counter C_1. Another counter, C_0, along with the storage register, provides the inputs to the comparator. When the contents of the storage register and counter C_0 are identical, the comparator generates a pulse. In a given spin period, the pulses generated by the comparator become a clock signal synchronized to the spin period. These pulses, along with the command reset pulse (command pulse), are used to reset counter C_0. Hence, they must be such that their action does not cause the loss of an f_0 count. This condition determines the pulse widths of the comparator-generated pulses and the command reset pulse; i.e., the command reset pulse is the leading edge of the centered sun pulse.

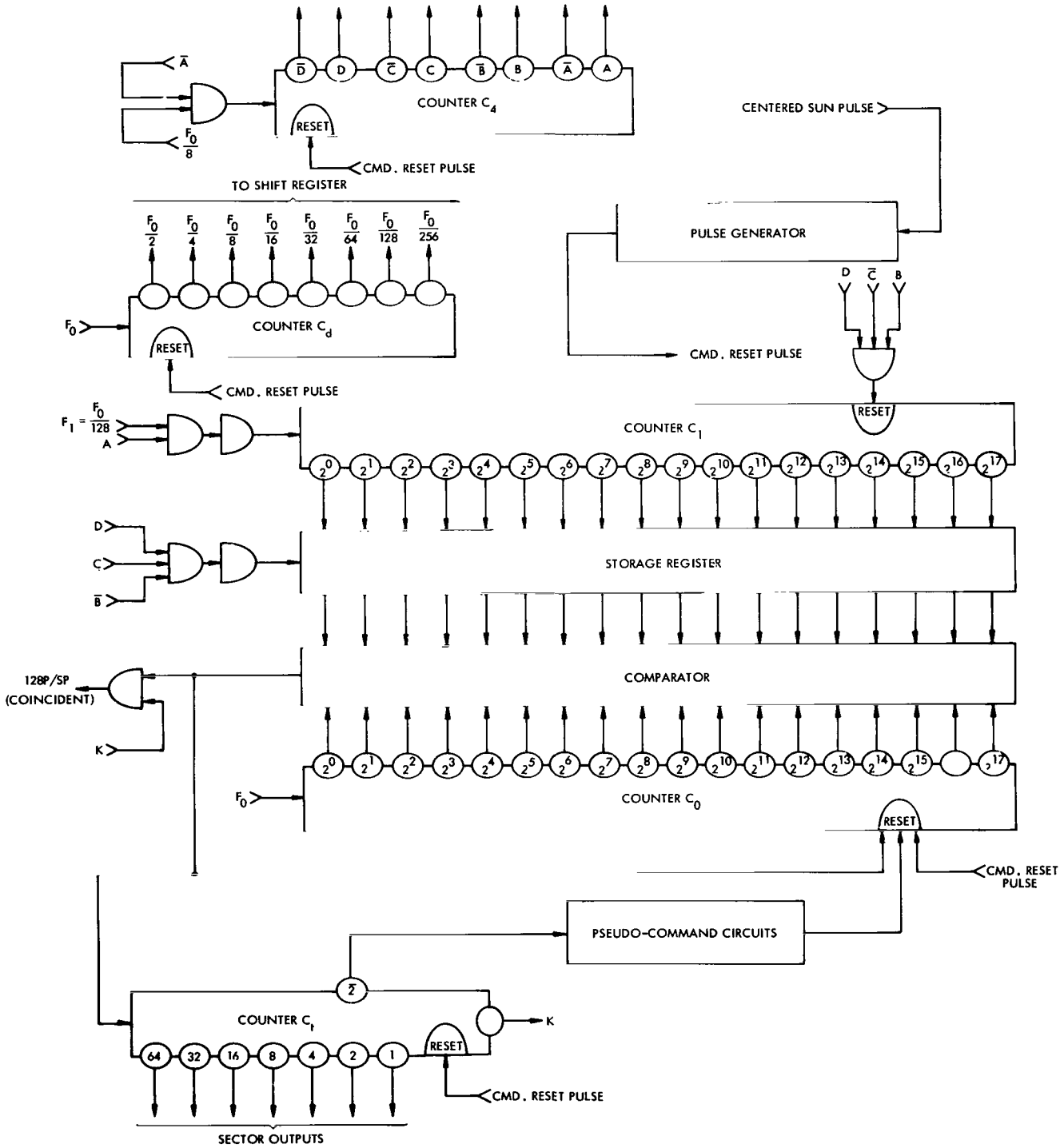

Figure 7—SSC block diagram.

The pulses generated by the comparator constitute the input signal to output counter C_t. Hence, decoding counter C_t provides information as to the instantaneous pointing direction of a point on the spacecraft.

During the rotation period, counter C_t should reach a count of 2^n (i.e., 128) and then be reset to zero by the command reset pulse.

If a command reset pulse does not occur after 2^n (i.e., 128) counts have been accumulated, the pseudo-command generator is activated, and the counter C_t overflows and starts accumulating counts again. When C_t next reaches 2^n (i.e., 128) counts and a command reset pulse has still not occurred, the pseudo-command generator produces a pseudo-command signal. This action continues, with a pseudo-command signal being generated every time C_t reaches 2^n (i.e., 128) counts. The occurrence of the command reset pulse causes C_t to be reset to zero and the pseudo-command generator to be deactivated. Hence, the output counter C_t will wait one spin period following the loss of the command reset pulse before generating a pseudo-command signal for every 2^n pulses from the comparator.

System Performance

The SSC divides the spin period into 2^n sectors. To accomplish this, it uses the information in the storage register as the basic interval to be sectored. An investigation of the accuracy of this information will lead to an evaluation of system performance.

Consider the representation of the spin period by interval counter C_1. This information may have a total error of minus one count of f_1. This follows directly from the division process performed in the generation of the f_1 signal. Since any division process can generate both a quotient and a remainder, the C_1 representation can differ from the true spin period by the amount of this remainder. This means that if the spin period is not an integer multiple of $T_1 = 1/f_1$, the contents of C_1 will be less than the spin period. This difference can be as small as 1 or as great as $2^n - 1$ counts of f_0.

Another consideration not previously mentioned is the interaction between the C_1 inhibit signal and the f_1 signal when spin period is measured. This effect may cause an extra count to be placed in counter C_1 if the inhibit signal occurs at a time when the f_1 signal is a "1". This occurs when the content of counter C_d is greater than one-half its capacity, i.e., when the last stage of C_d is a "1".

The combined effect of these two considerations is to incorporate a round-off error into interval counter C_1. If the remainder of the division process is less than 1/2, the interval counter contains only the number of counts of f_1 that occurred during the spin period. If the remainder is equal to or greater than 1/2 of f_1, the interval counter contains a count greater by 1 than the number of counts of f_1 sampled during the spin period. Hence, the error in the interval counter has been translated from a count of −1 to a count of ±1/2 of f_1. The total error in C_1 as a function of the remainder in C_d is shown in Figure 8. Thus when the remainder is less than 1/2 of f_1, the output counter attains a 2^n count before the next SSC command pulse. The maximum value of this time lapse is equal to $T_1/2$.

Another factor affecting system performance is the variation in two successive spin-period intervals. This variation may result either from a jitter effect of the onboard instrument's generating the

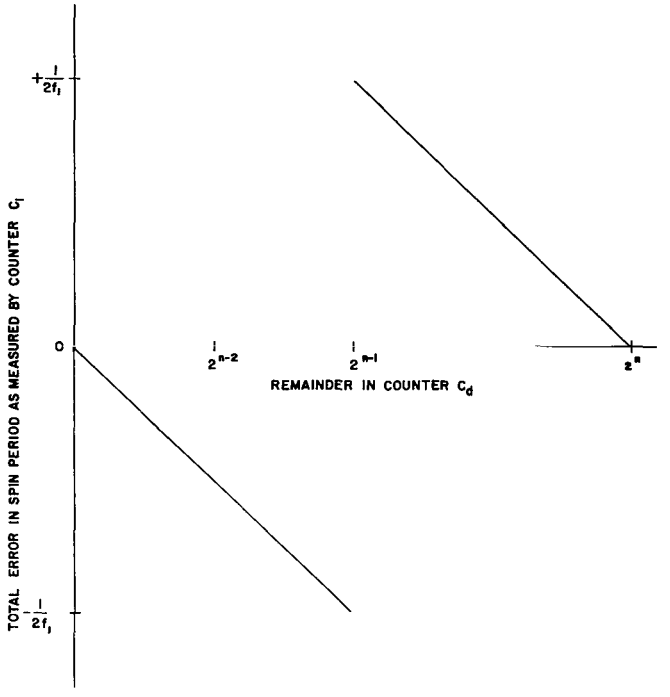

Figure 8—Total error in C_1 as a function of the remainder in C_d.

command pulse or directly from the motion of the spacecraft (precession). Since the operation of the SSC is based on the assumption that two successive spin periods are equal, this spin-period fluctuation has a one-to-one effect on system performance. However, this effect simply reduces the accuracy of the location of the sector pulses in a given spin interval.

A companion factor to the above short-term fluctuation is the long-term loss of the command pulse. This effect is taken into account in the operation of output counter C_t. Counter C_t operates in such a manner that, if the command pulse does not occur after 2^n pulses, the counter will continue to count until either 2^{n+1} counts have been registered or the command pulse occurs. When 2^{n+1} counts have been accumulated, the associated circuitry generates a pseudo-command signal. This signal resets continuous counter C_0 but does not update interval counter C_1. Therefore, the system waits one rotation period following the loss of the command pulse before generating a pseudo-command signal at the last known spin-period interval stored in the storage register. Hence, for a long-term loss of the command pulse the system continues to operate, but with the last known spin-period measurement.

Sector Determination: Location and Width

In order to define the location in a given spin period of a specific sector region, a reference system must first be considered. Let the reference system be based on the 360 degrees of rotation in a spin period. (See Figure 9.) Then, each pulse generated by the comparator and defining the end of a sector region is separated from the previous one by $360/2^n$ degrees of rotation. Hence, in this reference

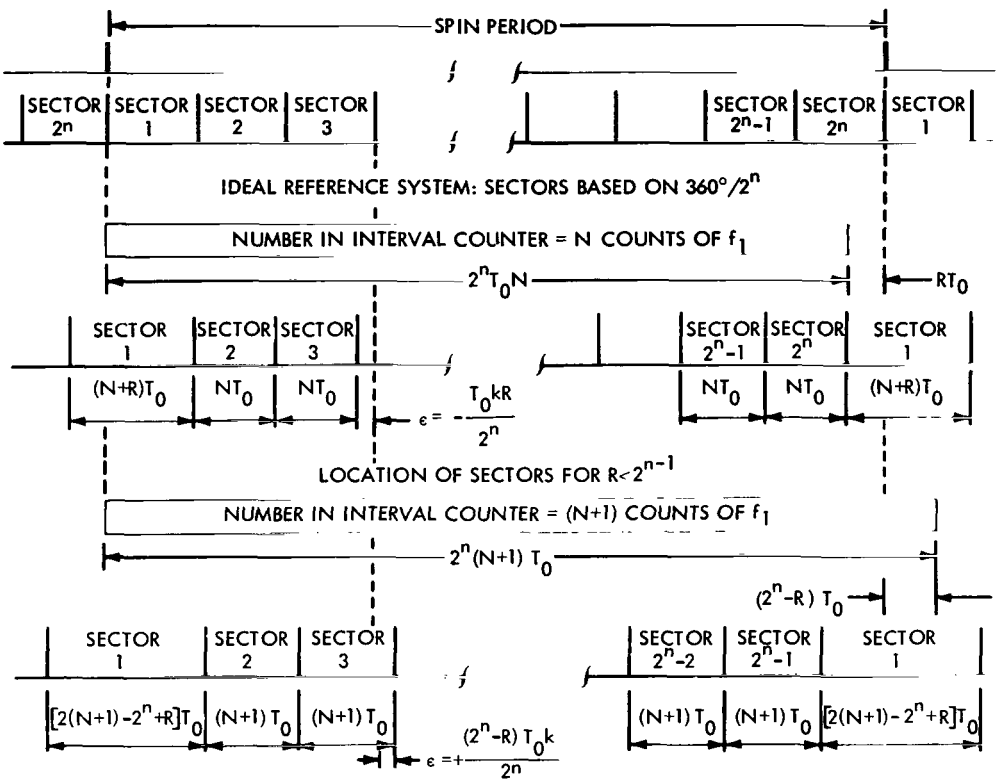

Figure 9—Sector determination.

system, the 2^n sector pulse occurs coincident with the command pulse, and the width of each sector is $360/2^n$ degrees.

The actual SSC generates sector pulses based on the spin-period representation present in the storage register. Hence, these sector pulses match the ideal reference system if, and only if, the remainder of the division process is equal to zero. In all other cases (where the remainder is greater than zero), the sector pulse generated by the comparator circuitry in the actual system is shifted from the reference system location by

$$\epsilon = \begin{cases} -\dfrac{T_0 R k}{2^n}, & \text{for } R < 2^{n-1} \\ +\dfrac{(2^n - R)T_0 k}{2^n}, & \text{for } R \geqslant 2^{n-1} \end{cases}$$

where

2^n = number of sector pulses in a spin,

$T_0 = 1/f_0$ = period of the f_0 signal,

R = remainder ($1 \leqslant R \leqslant 2^n - 1$),

and

k = number of the sector ($1, 2, 3, \ldots 2^n - 1, 2^n$).

Now examine the case for $R < 2^{n-1}$, the case when the remainder is less than 1/2 of f_1. The storage register contains a time representation of the spin period which is less than the actual value. Hence, the interval being divided into 2^n sectors is equal to the true spin period minus the time represented by the remainder (see storage register in Figure 7). Let

N = number of counts in interval counter C_1.

Then,

$(2^nN + R)T_0$ = true spin period,

2^nT_0N = time representation of spin period by storage register,

and

$T_0 = 1/f_0$.

Therefore, each sector pulse is generated slightly before the location of its corresponding ideal reference sector pulse. This effect is accumulative and results in the 2^nth sector pulse being generated T_0R seconds before the 2^n ideal reference sector pulse. Since each sector pulse resets continuous counter C_0, this counter will have obtained a value of R counts when the command pulse occurs.

Hence, if the first sector is defined as the time interval between the command pulse and the next pulse generated by the comparator, this results in an effective "dead time" between the end of the 2^nth sector and the start of the first sector in the next spin. That is,

$$\left.\begin{array}{l}\text{dead time width} = RT_0 \\ \text{sector width} = NT_0\end{array}\right\} R < 2^{n-1}.$$

Therefore, the time between the 2^nth sector pulse and the first sector pulse in the next spin will include the dead time and have a value of $(N + R)T_0$.

When $R \geqslant 2^{n-1}$ the information in the storage register represents the true spin period plus the effect of the inhibit signal adding a count to the interval counter C_1. This increases the contents of counter C_1 by 1; so N is replaced by $N + 1$.

We have

$(2^nN + R)T_0$ = true spin period

and

$2^n(N + 1)T_0$ = time representation of the spin period by storage register.

Hence, it is the quantity $2^n(N + 1)T_0$ that is divided by 2^n. This results in each sector pulse being generated by the comparator slightly after its corresponding ideal reference sector pulse. Again this effect is accumulative and the 2^nth sector pulse should occur a $(2^n - R)T_0$ time interval after its ideal reference sector pulse. This time is also after the command pulse which resets both the continuous and

output counters. Hence, the system will reset before the generation of the 2^nth sector pulse. Hence, the comparator will generate $2^n - 1$ pulses in a given spin period. That is,

$$\left.\begin{aligned}\text{dead time width} &= (2^n - R)T_0 \\ \text{sector width} &= (N+1)T_0\end{aligned}\right\} R \geqslant 2^{n-1}.$$

Again, the dead time width is included between the $2^n - 1$ sector pulse and the first sector pulse in the next spin. This internal, referred to as the width of sector 1, will have a value of $[2(N+1) - (2^n - R)]T_0$.

Hence, the location of each sector pulse and the width of each sector can be determined from knowledge of the spin period and remainder values.

Operating Range: f_0, 2^n, and Spin Rate ω_z

The operating range of the SSC is determined by the relationship between f_0 in Hz, 2^n, and the spin rate of the spacecraft ω_z in rpm. As previously mentioned, the division process can generate both a quotient and a remainder. The effect of the remainder is to shift the sector pulse from its reference location. The maximum shift occurs in the 2^n sector and has a value of RT_0. Hence, if R is greater than the number of counts that represents the spin period in interval counter C_1, the shift caused by R may be greater than a sector width. Therefore, one constraint on the relationship between f_0, 2^n, and spin rate is that the number of pulses in interval counter C_1 be equal to or greater than remainder R. We have

$$R_{\max} = 2^n - 1$$

and

$$N_{ic} \geqslant 2^n,$$

where N_{ic} is the number of pulses fed into interval counter C_1.

Since the number of pulses N_{ic} fed into the interval counter C_1 is a result of frequency division by 2^n, the minimum number of pulses N_{id} fed into frequency-divider counter C_d must satisfy

$$N_{id} \geqslant 2^n N_{io},$$

where N_{io} is the number of pulses out of counter C_d. Therefore,

$$N_{id} = \frac{\text{spin period}}{T_0} = \frac{60f_0}{\omega_z},$$

$$N_{id} = N_{ic},$$

$$N_{id} \geqslant 2^n N_{ic} \geqslant 2^{2n},$$

$$\frac{60f_0}{\omega_z} \geqslant 2^{2n},$$

and

$$f_0 \geqslant \frac{2^{2n}\omega_z}{60}.$$

A further constraint on the operating range of the SSC is that the number of pulses into the interval counter, N_{ic}, must not exceed its capacity. Thus,

$$2^k = \text{capacity of interval counter } C_1 \ (k = 17),$$

$$N_{ic} < 2^k,$$

and

$$N_{io} < 2^k,$$

and, since

$$N_{io} < \frac{N_{id}}{2^n}$$

and

$$N_{id} = \frac{60 f_0}{\omega_z},$$

we have

$$2^n \frac{60 f_0}{\omega_z} < 2^k$$

and

$$f_0 < \frac{2^{n+k}\omega_z}{60}.$$

Consideration of both constraints yields

$$\frac{2^{2n}\omega_z}{60} \leqslant f_0 < \frac{2^{n+k}\omega_z}{60}.$$

System Output Signals

The comparator generates the basic clock signal synchronized to spin rate. As previously mentioned, this signal is subject to the effect of the remainder value, which causes noncoincidence of the 2^nth (i.e., 128th) pulse and the command reset pulse. Therefore, logic is provided to delete the 128th pulse from this signal and replace it with the command reset pulse. This results in the basic clock signal's having coincidence of the last pulse and the command reset pulse, independent of the remainder value. It is this coincident 128-pulse signal that is sent to the experimenter. (See Figures 10A and 10B.)

The output of each stage of output counter C_t is also available to all spacecraft systems. Separate buffering is supplied for each actual interface, and a special interface exists between the SSC and the spacecraft encoder.

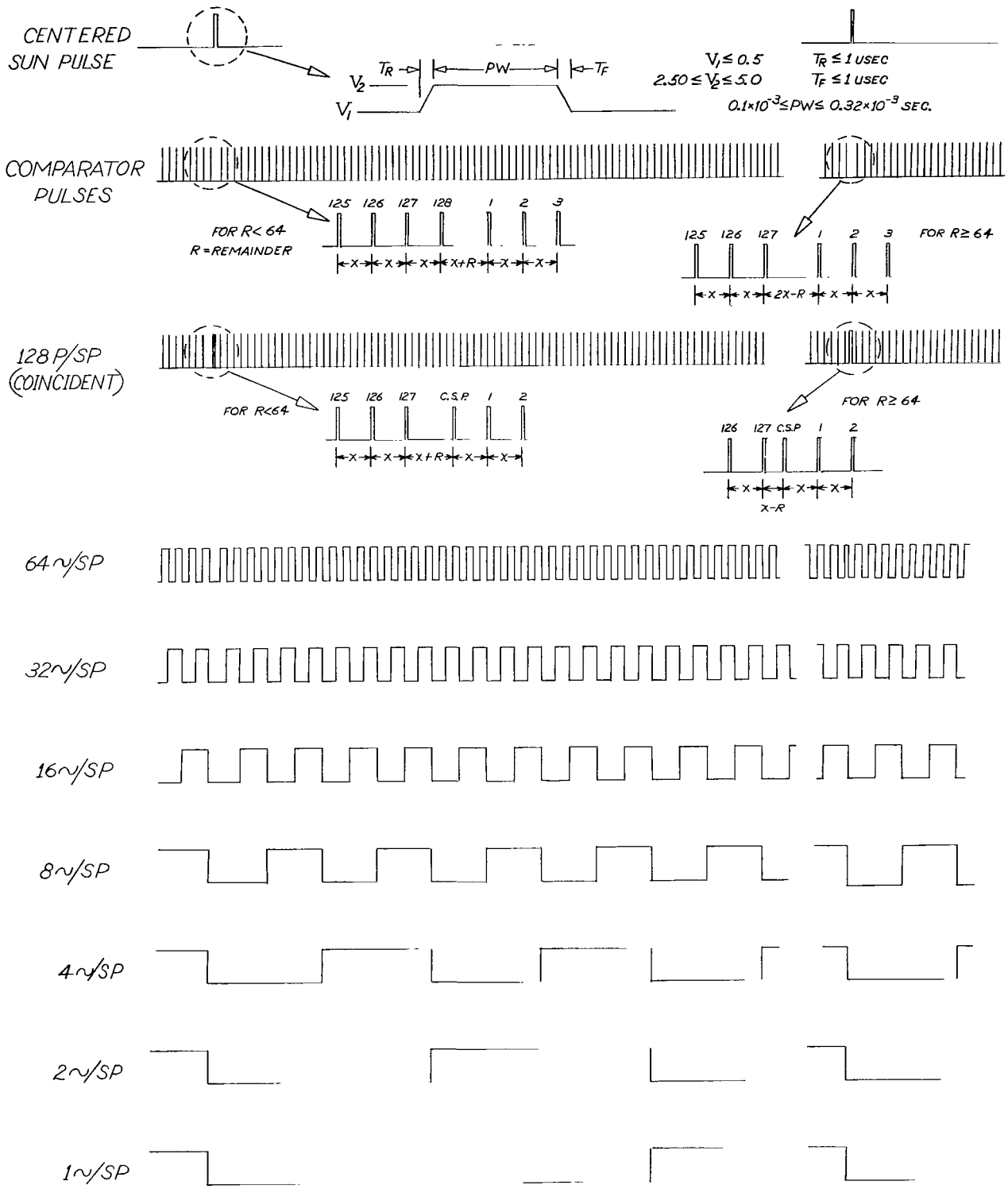

Figure 10A—SSC output signals, basic logic.

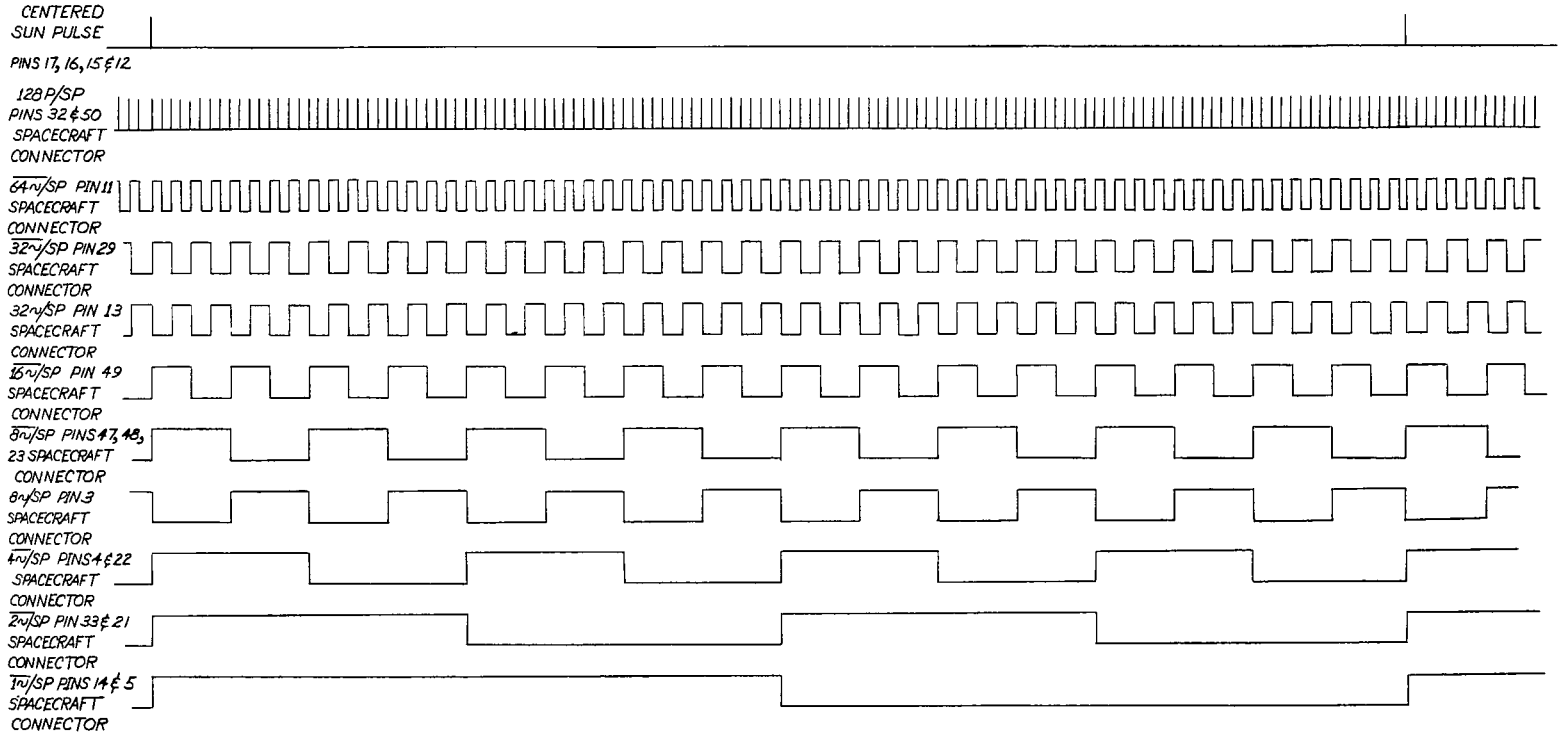

UNIV. OF CHICAGO	PIN 3 & PIN 17
A.E.C. LOS ALAMOS	PIN 11, PIN 29 & PIN 49
A.C.S. ELECTRONICS	PIN 14, PIN 33, PIN 22, PIN 47, PIN 16
SOLAR ELECTRONICS	PIN 50
PLASMA	PIN 32 & PIN 15
ELECTRIC FIELDS	PIN 13 & PIN 37

Figure 10B—SSC output signals, connector details.

Goddard Space Flight Center
National Aeronautics and Space Administration
Greenbelt, Maryland, July 13, 1970
861-51-75-01-51

Appendix A

THEORETICAL CONSIDERATIONS OF ASPECT DETERMINATION

Energy and Momentum Considerations

In the solution to the problem of force-free motion of a rigid body, a point on the body can be defined in terms of the body-fixed axes, x, y, and z. For the purpose of defining the orientation of the body fixed axes relative to nonrotating reference axes, X, Y, and Z, Euler introduced three independent angles, ϕ, ψ, and θ. These Eulerian angles are shown in Figure A-1 and are defined by three successive rotations performed in a specific sequence. The sequence is started by (1) rotation of the initial set of axes X, Y, and Z, counterclockwise about the Z-axis through an angle ϕ, producing the intermediate set of axes, ξ', η', and ζ' (Figure A-1a). (2) Next, this intermediate set of axes is rotated counterclockwise through an angle θ about the ξ'-axis, producing a second intermediate set of axes, ξ, η, and ζ (Figure A-1b). The ξ'-axis is also called the line of nodes. (3) Finally, axes ξ, η, and ζ are rotated counterclockwise about the ζ-axis through an angle ψ, forming axes x, y, and z (Figure A-1c). Hence, the Eulerian angles, ϕ, ψ, and θ, completely describe the orientation of the x, y, z coordinate system with respect to the X, Y, Z coordinate system.

A mathematical method of representing the rotations described above and based on the matrix representation of an orthogonal transformation is given in Appendix B.

Now let the X, Y, Z coordinate system define an inertial space. Assume a rotating spacecraft situated in this inertial space where the momentum vector, **L**, of the spacecraft is orientated along the Z-axis of the defining coordinate system. Let the x, y, z coordinate system be aligned with the three principle moments of inertia of the spacecraft, I_1, I_2, and I_3. Hence, the x, y, z system is fixed in the rotating spacecraft. The instantaneous values of momentum about axes x, y, and z are, respectively,

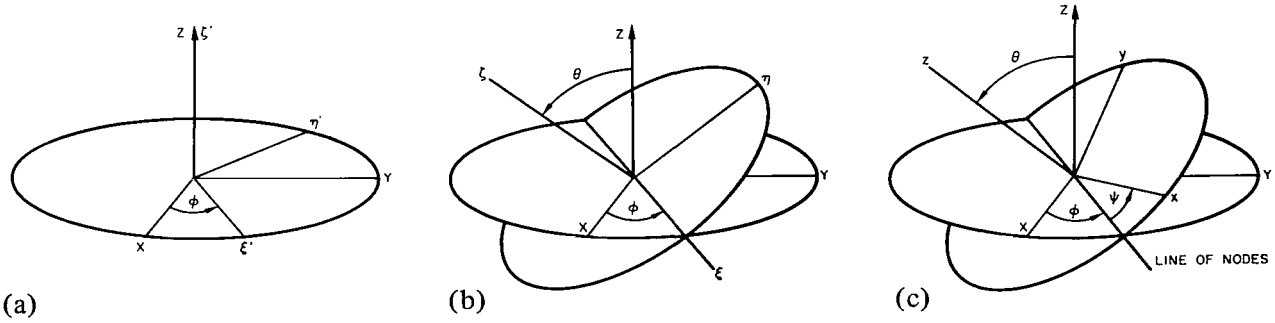

Figure A-1—Euler's rotation angle.

$$p_x = I_1 \omega_x \,, \tag{A-1}$$

$$p_y = I_2 \omega_y \,, \tag{A-2}$$

and

$$p_z = I_3 \omega_z \,, \tag{A-3}$$

where ω_x, ω_y, and ω_z are the respective instantaneous values of angular velocity about axes x, y, and z. The respective instantaneous values of the momentum p_x, p_y, p_z and the angular velocity ω_x, ω_y, ω_z about the x, y, and z axes can be expressed in terms of the momentum vector (see Figure A-2 and Appendix C):

$$p_x = L \sin\theta \sin\psi \,, \tag{A-4}$$

$$p_y = L \sin\theta \cos\psi \,, \tag{A-5}$$

$$p_z = L \cos\theta \,, \tag{A-6}$$

$$\omega_x = \dot{\phi} \sin\psi \sin\theta + \dot{\theta} \cos\psi \,, \tag{A-7}$$

$$\omega_y = \dot{\phi} \cos\psi \sin\theta - \dot{\theta} \sin\psi \,, \tag{A-8}$$

and

$$\omega_z = \dot{\phi} \cos\theta + \dot{\psi} \,. \tag{A-9}$$

Substitution of Equations A-4 through A-9 in Equations A-1 through A-3 yields

$$p_x = L \sin\psi \sin\theta = I_1(\dot{\phi} \sin\psi \sin\theta + \dot{\theta} \cos\psi) \,, \tag{A-10}$$

$$p_y = L \cos\psi \sin\theta = I_2(\dot{\phi} \cos\psi \sin\theta - \dot{\theta} \sin\psi) \,, \tag{A-11}$$

and

$$p_z = L \cos\theta = I_3(\dot{\phi} \cos\theta + \dot{\psi}) \,. \tag{A-12}$$

Multiplying Equation A-10 by sin ψ and Equation A-11 by cos ψ and adding the results gives

$$L \sin\theta = (I_1 - I_2)\dot{\theta} \cos\psi \sin\psi + \dot{\phi} \sin\theta(I_1 \sin^2\psi + I_2 \cos^2\psi) \,. \tag{A-13}$$

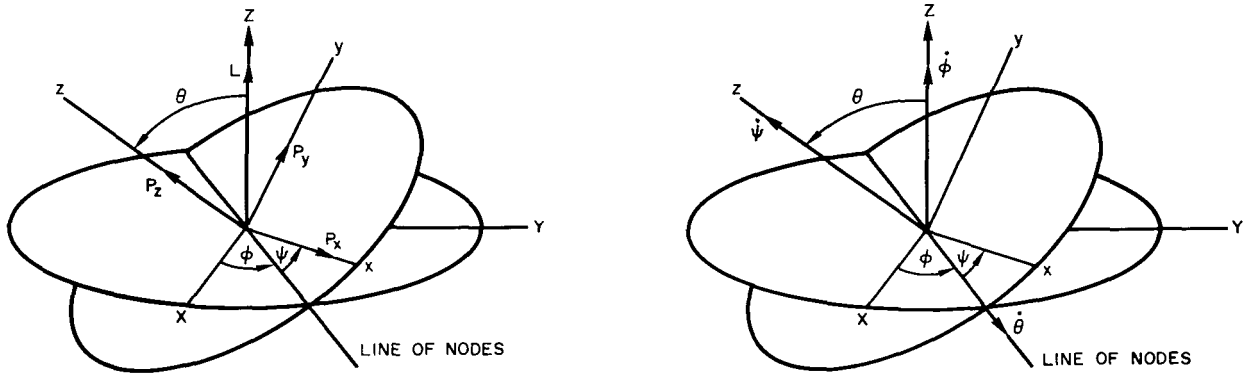

Figure A-2—Components of angular momentum and velocities.

Multiplying Equation A-10 by cos ψ and Equation A-11 by sin ψ and subtracting the results gives

$$0 = \dot{\phi} \cos \psi \sin \psi \sin \theta (I_1 - I_2) + \dot{\theta}(I_1 \cos^2 \psi + I_2 \sin^2 \psi) . \tag{A-14}$$

If the spacecraft is assumed to be dynamically balanced about the z-axis, then $I_1 = I_2$. Making this assumption and substituting in Equations A-13 and A-14, we obtain

$$L = I_1 \dot{\phi} \tag{A-15}$$

and

$$I_1 \dot{\theta} = 0 . \tag{A-16}$$

Since $I_1 \neq 0$, $\dot{\theta}$ must be zero; it follows that θ is independent of time. Substitution of Equations A-15 and A-16 in Equation A-12 yields

$$p_z = I_1 \dot{\phi} \cos \theta = I_3(\dot{\phi} \cos \theta + \dot{\psi}) . \tag{A-17}$$

Solving for $\dot{\psi}$, the angular velocity of the spacecraft about the spacecraft z-axis, we obtain

$$\dot{\psi} = \frac{(I_1 - I_3)\dot{\phi} \cos \theta}{I_3} . \tag{A-18}$$

Solving for $\dot{\phi}$, the angular velocity of the spacecraft z-axis about the momentum vector or, more precisely, the angular velocity of the line of nodes, we obtain

$$\dot{\phi} = \frac{I_3 \dot{\psi}}{(I_1 - I_3) \cos \theta} . \tag{A-19}$$

Let us refer to $\dot{\phi}$ as precession rate and $\dot{\psi}$ as the spin rate (to be distinguished from the apparent rotation rate of the spacecraft with respect to a fixed external point). (Note that by Equation A-9, $\omega_z = \dot{\psi}$ when $\dot{\phi} = 0$.) This apparent rotation rate has an average value of $\dot{\phi} + \dot{\psi}$. The precession cone half angle is θ, and the rate of change of the precession cone half angle is $\dot{\theta}$. If $I_1/I_3 < 1$, θ tends toward zero, and the precession coning will damp out in time. Since it is usually desirable for the satellite to rotate about the z-axis, most spin-stabilized satellites are balanced so that the z-axis coincides with the largest moment of inertia. The rest of this text will deal only with this case, resulting in the fact that $\theta = 0$. It should not be assumed that zero precession implies that $\dot{\phi}$ goes to zero. Equation A-19 states that when $\theta = 0$, then $\dot{\phi} = I_3\dot{\psi}/(I_1 - I_3)$.

Equations Determining Spacecraft Aspect

Figure A-3 shows the spacecraft momentum vector relative to the sun and zenith vector on the celestial sphere (which is centered at the spacecraft's center of mass). The zenith vector is defined as a vector from the earth's center through the spacecraft's center of mass. The earth's center is located on the celestial sphere at $(RA_z + 180)$ and $(-D_z)$, where RA_z is the right ascension and D_z is the declination of the zenith vector. The great-circle arc from the sun to the zenith vector is η. Applying the laws of sines and cosines to the spherical triangles in Figure 3, we write the equations for the values of η and the angles $\angle 1$ and $\angle 3$ as

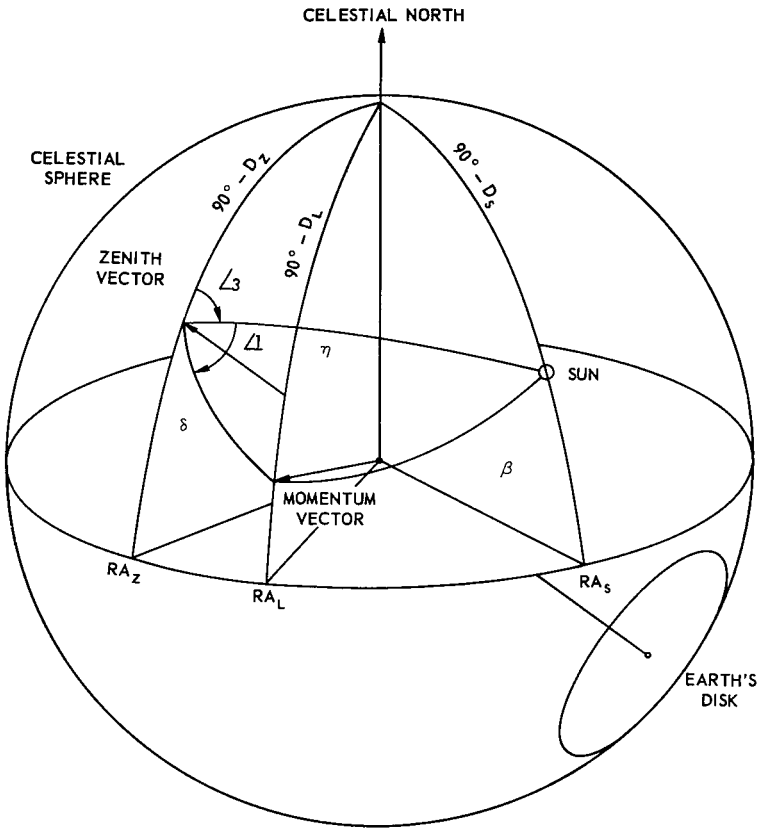

Figure A-3—Spacecraft momentum vector relative to the sun and the zenith vector.

$$\cos \eta = \sin D_z \sin D_s + \cos D_z \cos D_s \cos (RA_s - RA_z) , \text{ if } 0 \leqslant \eta < 180^\circ ,$$

$$\cos \angle 1 = \frac{\cos \beta - \cos \eta \cos \delta}{\sin \eta \sin \delta} ,$$

$$\sin \angle 1 = \frac{\sin \beta \sin \angle 2}{\sin \eta} ,$$

$$\cos \angle 3 = \frac{\sin D_s - \cos \eta \sin D_z}{\sin \eta \cos D_z} ,$$

and

$$\sin \angle 3 = \frac{\sin (RA_s - RA_z) \cos D_s}{\sin \eta} ,$$

where β is the angle between the sun and the momentum vector (spin axis) and δ is the angle between the zenith and momentum vectors. Using the above values of $\angle 1$ and $\angle 3$, we can derive the right ascension RA_L and declination D_L of the momentum vector:

$$\sin D_L = \sin D_z \cos \delta + \cos D_z \sin \delta \cos (\angle 3 + \angle 1) , \text{ if } 90° < D_L \leqslant 90° ,$$

$$\cos (RA_L - RA_z) = \frac{\cos \delta - \sin D_z \sin D_L}{\cos D_z \cos D_L} ,$$

$$\sin (RA_L - RA_z) = \frac{\sin (\angle 1 + \angle 3) \sin \delta}{\cos D_L} ,$$

and

$$RA_L = RA_z + (RA_L - RA_z) .$$

Therefore, to derive the right ascension and declination of the spacecraft's momentum vector, we must know several quantities. The right ascensions and declinations of the zenith vector (RA_z, D_z) and the sun (RA_s, D_s) are accurately known from earth-based information, whereas β, δ, and $\angle 2$ must be determined on board the spacecraft. From Figure A-3 it is clear (since apparent rotation rate is $\dot{\phi} + \dot{\psi}$) that

$$\angle 2 = (\dot{\phi} + \dot{\psi})\Delta t_c \pm 180° , \tag{A-20}$$

where Δt_c is the time required for the reference plane to move from the sun to the earth's center. Therefore, it is the measurement of β, δ, and $(\dot{\phi} + \dot{\psi})\Delta t_c$ that the aspect system must perform.

Appendix B

MATHEMATICAL REPRESENTATION OF EULERIAN ROTATIONS

Any vector **N** in the X, Y, Z coordinate system, written in column form, may be transformed into the ξ', η', ζ' system by the application of the rotation matrix D:

$$\begin{vmatrix} N_{\xi'} \\ N_{\eta'} \\ N_{\zeta'} \end{vmatrix} = D \begin{vmatrix} N_X \\ N_Y \\ N_Z \end{vmatrix} = \begin{vmatrix} \cos\phi & \sin\phi & 0 \\ -\sin\phi & \cos\phi & 0 \\ 0 & 0 & 1 \end{vmatrix} \begin{vmatrix} N_X \\ N_Y \\ N_Z \end{vmatrix}.$$

This vector, when acted upon by the rotation matrix C, yields

$$\begin{vmatrix} N_\xi \\ N_\eta \\ N_\zeta \end{vmatrix} = CD \begin{vmatrix} N_X \\ N_Y \\ N_Z \end{vmatrix} = \begin{vmatrix} 1 & 0 & 0 \\ 0 & \cos\theta & \sin\theta \\ 0 & -\sin\theta & \cos\theta \end{vmatrix} \begin{vmatrix} \cos\phi & \cos\phi & 0 \\ -\sin\phi & \cos\phi & 0 \\ 0 & 0 & 1 \end{vmatrix} \begin{vmatrix} N_X \\ N_Y \\ N_Z \end{vmatrix}.$$

Finally, application of the rotation matrix B produces the N vector transformed to the x, y, z coordinate system:

$$\begin{vmatrix} N_x \\ N_y \\ N_z \end{vmatrix} = BCD \begin{vmatrix} N_X \\ N_Y \\ N_Z \end{vmatrix} = \begin{vmatrix} \cos\psi & \sin\psi & 0 \\ -\sin\psi & \cos\psi & 0 \\ 0 & 0 & 1 \end{vmatrix} \begin{vmatrix} 1 & 0 & 0 \\ 0 & \cos\theta & \sin\theta \\ 0 & -\sin\theta & \cos\theta \end{vmatrix} \begin{vmatrix} \cos\phi & \sin\phi & 0 \\ -\sin\phi & \cos\phi & 0 \\ 0 & 0 & 1 \end{vmatrix} \begin{vmatrix} N_X \\ N_Y \\ N_Z \end{vmatrix}.$$

Hence, any vector in the X, Y, Z coordinate system can be determined in the x, y, z coordinate system by the application of the transformation matrix $A = BCD$. Performing the matrix multiplication, we obtain

$$A = \begin{vmatrix} \cos\psi\cos\phi - \cos\theta\sin\phi\sin\psi & \cos\psi\sin\phi + \cos\theta\cos\phi\sin\psi & \sin\psi\sin\theta \\ -\sin\psi\cos\phi - \cos\theta\sin\phi\cos\psi & -\sin\psi\sin\phi + \cos\theta\cos\phi\cos\psi & \cos\psi\sin\theta \\ \sin\theta\sin\phi & -\sin\theta\cos\phi & \cos\theta \end{vmatrix}. \qquad \text{(B-1)}$$

Since A is an orthogonal transformation, then $A^{-1} = A^T$, and any vector in the x, y, z system can be transformed to the X, Y, Z system by application of the transformation matrix A^{-1}, we have

$$A^{-1} = \begin{vmatrix} \cos\phi\cos\psi - \sin\phi\cos\theta\sin\psi & -\sin\psi\cos\phi - \cos\theta\cos\psi\sin\phi & \sin\theta\sin\phi \\ \sin\phi\cos\psi + \cos\theta\cos\phi\sin\psi & -\sin\psi\sin\phi + \cos\theta\cos\psi\cos\phi & -\sin\theta\cos\phi \\ \sin\theta\sin\psi & \sin\theta\cos\psi & \cos\theta \end{vmatrix}.$$

Appendix C

MOMENTUM AND ANGULAR VELOCITIES

Momentum

Consider the momentum vector **L** of a rotating spacecraft oriented along the Z-axis of the X, Y, Z coordinate system. (See Figure A-2a.) Writing the momentum vector as a column vector in the X, Y, Z system, we have

$$\mathbf{L} = \begin{vmatrix} L_X \\ L_Y \\ L_Z \end{vmatrix} = \begin{vmatrix} 0 \\ 0 \\ L \end{vmatrix}.$$

Hence, transforming the momentum vector to the x, y, z coordinate system, we obtain the instantaneous values of momentum about the x, y, and z axes. Denoting these values as p_x, p_y, and p_z, respectively, we have (because A is defined as in Equation B-1)

$$\begin{vmatrix} p_x \\ p_y \\ p_z \end{vmatrix} = AL = A \begin{vmatrix} 0 \\ 0 \\ L \end{vmatrix} = \begin{vmatrix} L \sin \psi \sin \theta \\ L \cos \psi \sin \theta \\ L \cos \theta \end{vmatrix}.$$

Therefore,

$$p_x = L \sin \psi \sin \theta ,$$

$$p_y = L \cos \psi \sin \theta ,$$

and

$$p_z = L \cos \theta .$$

Angular Velocities

Consider $\omega_\phi = d\phi/dt = \dot{\phi}$ as vector directed along the Z-axis (see Figure A-2b). Writing ϕ as a column vector, we obtain

$$\dot{\phi} = \begin{vmatrix} 0 \\ 0 \\ \dot{\phi} \end{vmatrix}.$$

Then, expressing $\dot{\phi}$ in the x, y, z coordinate system we have

$$\begin{vmatrix} \omega_{\phi_x} \\ \omega_{\phi_y} \\ \omega_{\phi_z} \end{vmatrix} = \begin{vmatrix} \dot{\phi}_x \\ \dot{\phi}_y \\ \dot{\phi}_z \end{vmatrix} = A\dot{\phi} = A \begin{vmatrix} 0 \\ 0 \\ \dot{\phi} \end{vmatrix} = \begin{vmatrix} \dot{\phi} \sin \psi \sin \theta \\ \dot{\phi} \cos \psi \sin \theta \\ \dot{\phi} \cos \theta \end{vmatrix};$$

thus,

$$\omega_{\phi_x} = \dot{\phi} \sin \psi \sin \theta,$$

$$\omega_{\phi_y} = \dot{\phi} \cos \psi \sin \theta,$$

and

$$\omega_{\phi_z} = \dot{\phi} \cos \theta.$$

Next, consider $\omega_\theta = d\theta/dt = \dot{\theta}$ as a vector directed along the line of nodes. Writing $\dot{\theta}$ as a column vector in the X, Y, Z system, we have

$$\dot{\theta} = \begin{vmatrix} \dot{\theta} \cos \phi \\ \dot{\theta} \sin \phi \\ 0 \end{vmatrix}.$$

Transforming this vector to the x, y, z system, we have

$$\begin{vmatrix} \omega_{\theta_x} \\ \omega_{\theta_y} \\ \omega_{\theta_z} \end{vmatrix} = \begin{vmatrix} \theta_x \\ \theta_y \\ \theta_z \end{vmatrix} = A\dot{\theta} = A \begin{vmatrix} \dot{\theta} \cos \phi \\ \dot{\theta} \sin \phi \\ 0 \end{vmatrix} = \begin{vmatrix} \dot{\theta} \cos \psi \\ -\dot{\theta} \sin \psi \\ 0 \end{vmatrix}.$$

Thus,

$$\omega_{\theta_x} = \dot{\theta} \cos \psi,$$

$$\omega_{\theta_y} = -\dot{\theta} \sin \psi,$$

and

$$\omega_{\theta_z} = 0.$$

Finally, consider $\omega_{\psi} = d\psi/dt = \dot{\psi}$ a vector perpendicular to the plane containing the line of nodes and the x-axis and directed along the z-axis. Hence,

$$\begin{vmatrix} \omega_{\psi_x} \\ \omega_{\psi_y} \\ \omega_{\psi_z} \end{vmatrix} = \begin{vmatrix} 0 \\ 0 \\ \dot{\psi} \end{vmatrix} .$$

Now, combining the x, y, and z components of $\dot{\phi}$, $\dot{\psi}$, and $\dot{\theta}$, we establish a relationship between the angular velocities ω_x, ω_y, and ω_z and the rate of change of the Euler angles:

$$\omega_x = \dot{\phi} \sin \psi \sin \theta + \dot{\theta} \cos \psi ,$$

$$\omega_y = \dot{\phi} \cos \psi \sin \theta - \dot{\theta} \sin \psi ,$$

and

$$\omega_z = \dot{\phi} \cos \theta + \dot{\psi} .$$

Appendix D

CALCULATION OF δ

The information contained in the relative position of the detector output pulses to the command-slit crossing of the sun provides a measure of δ, the inclination of the spacecraft zenith vector to the spin axis. Consider the celestial sphere shown in Figure D-1 with the spacecraft located at the center of the sphere. The arc length X_1 is the smaller of the two possible great-circle arc distances from the sun to the horizon. From spherical trigonometry it follows that

$$\cos X_1 = \cos\beta \cos\gamma + \sin\beta \sin\gamma \cos A .$$

There are two values of X_1 that satisfy this equation. This ambiguity can be removed if the magnitude of angle A is taken into account:

$$\text{If } \pi - A > 0 , \text{ then } 0 \leqslant X_1 < \pi .$$

$$\text{If } \pi - A < 0 , \text{ then } \pi < X_1 \leqslant 2\pi .$$

$$\text{If } \pi - A = 0 , \text{ then } X_1 = \beta + \gamma .$$

Angle A corresponds to the relative position of the earth's horizon with respect to the command-slit crossing of the solar disk. Hence, X_1 is uniquely determined, and

$$\sin X_1 = \sqrt{1 - \cos^2 X_1} .$$

Now, applying the cosine and sine laws of spherical trigonometry to the triangle containing the angle X_2, we have

$$\cos X_2 = \frac{\cos\beta - \cos X_1 \cos\gamma}{\sin X_1 \sin\gamma}$$

and

$$\sin X_2 = \sin\beta \frac{\sin A}{\sin X_1} .$$

Therefore, X_2 is also uniquely determined.

Let r_e equal the mean radius of the earth and h be the height of the satellite above the earth (see Figure D-2c). Then,

$$\sin\rho = \frac{r_e}{r_e + h} \quad (0 \leqslant \rho < 90^\circ) ,$$

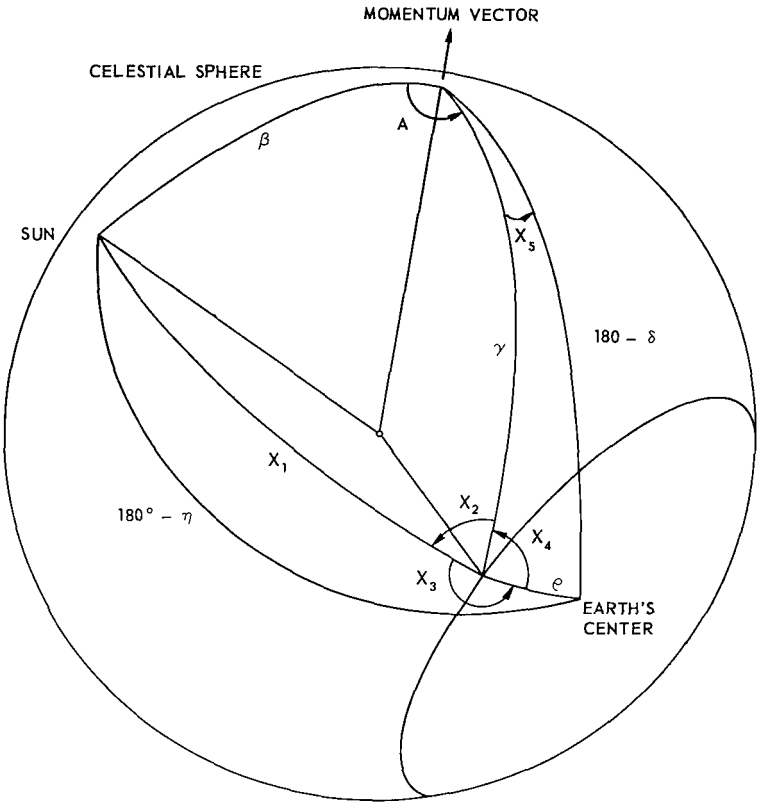

Figure D-1—Celestial sphere representation of the single horizon solution for δ.

and, from Figure D-1,

$$\cos X_3 = \frac{-\cos \eta - \cos X_1 \cos \rho}{\sin X_1 \sin \rho} .$$

Again there are two values of X_3 that satisfy this equation. Also, from Figure D-1,

$$X_4 = 2\pi - (X_2 \pm X_3) ,$$

and X_4 has two possible values corresponding to the two values of X_3. Also,

$$\cos \delta = -\cos \rho \cos \gamma - \sin \rho \sin \gamma \cos X_4 \quad (0 \leqslant \delta < 180°) , \tag{D-1}$$

and δ is doubled-valued.

The information contained in the spacing of the horizon-detector output pulses and the relative position of the earth's center from the sun provide alternate methods for δ calculation.

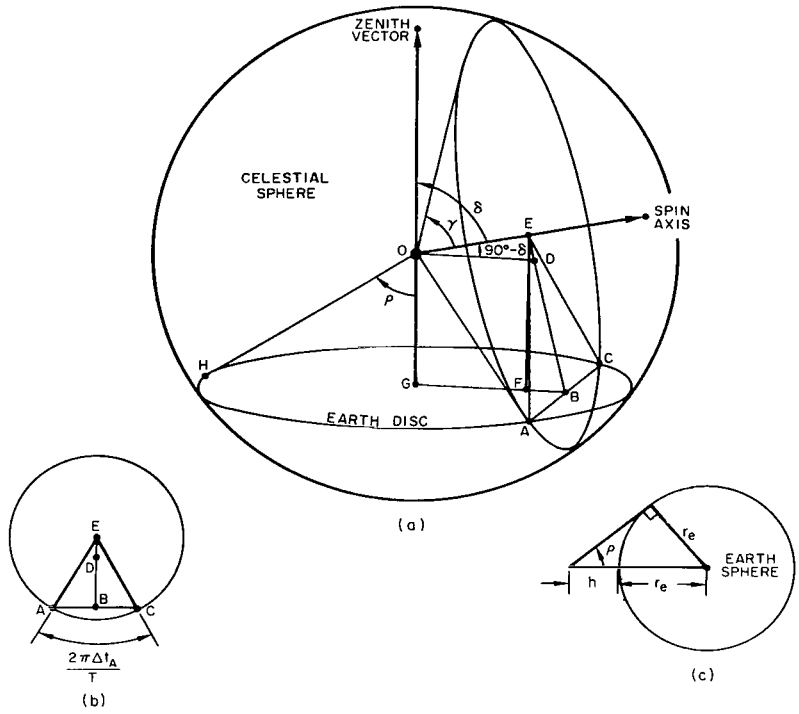

Figure D-2—Definition of variables for the two horizon solution for δ.

Referring to Figure D-2b and considering the plane containing EA and EC, we have

$$\cos\frac{\pi\Delta t_a}{T_E} = \frac{EB}{EA}, \tag{D-2}$$

where Δt_a is the time between horizon pulses, and T_E is the rotation period. From Figure D-2, various other relationships can be derived:

$$EB = ED + DB, \tag{D-3}$$

$$ED = OE \tan(90 - \delta), \text{ where } OE = OA \cos\gamma = OH \cos\gamma, \tag{D-4}$$

$$DB = \frac{OG}{\cos(90 - \delta)}, \qquad \text{where } OG = OH \cos\rho, \tag{D-5}$$

$$EA = OA \sin\gamma = OH \sin\gamma, \tag{D-6}$$

and

$$ED = OH \cos\gamma \tan(90 - \delta).$$

From Equation D-5,

$$DB = \frac{OH \cos \rho}{\cos (90 - \delta)}.$$

Hence, from Equation D-2,

$$EB = OH \cos \gamma \tan (90 - \delta) + \frac{OH \cos \rho}{\cos (90 - \delta)},$$

$$= OH\left(\cos \gamma \cot \delta + \frac{\cos \rho}{\sin \delta}\right).$$

Thus, from Equation D-2,

$$OH\left(\cos \gamma \cot \delta + \frac{\cos \rho}{\sin \delta}\right) = EA \cos \frac{\pi \Delta t_a}{T_E}. \tag{D-7}$$

Then, from Equation D-6,

$$OH \cos \gamma \cot \delta + \frac{\cos \rho}{\sin \delta} = OH \sin \gamma \cos \frac{\pi \Delta t_a}{T_E}. \tag{D-8}$$

Therefore,

$$\sin \delta \cos \gamma \cot \delta + \cos \rho = \sin \delta \sin \gamma \cos \frac{\pi \Delta t_a}{T_E}; \tag{D-9}$$

that is,

$$\cos \gamma \cos \delta + \cos \rho = \sin \delta \sin \gamma \cos \frac{\pi \Delta t_a}{T_E}. \tag{D-10}$$

Let

$$d = \cos \rho,$$

$$\epsilon = \cos \gamma,$$

and

$$f = \sin \gamma \cos \frac{\pi \Delta t_a}{T_E}.$$

Then,

$$d + \epsilon \cos \delta = f \sin \delta = f\sqrt{1 - \cos^2 \delta}. \tag{D-11}$$

Squaring both sides, we have

$$d^2 + 2\epsilon d \cos \delta + \epsilon^2 \cos^2 \delta + f^2 \cos^2 \delta - f^2 = 0,$$

or

$$(\epsilon^2 + f^2) \cos^2 \delta + 2\epsilon d \cos \delta + (d^2 - f^2) = 0. \tag{D-12}$$

Thus,

$$\cos\delta = \frac{-\epsilon d \pm \sqrt{d^2\epsilon^2 - (\epsilon^2 + f^2)(d^2 - f^2)}}{\epsilon^2 + f^2};$$

that is,

$$\cos\delta = \frac{-d\epsilon \pm f\sqrt{\epsilon^2 + f^2 - d^2}}{\epsilon^2 + f^2}.$$

Figure D-2 represents a spacecraft rotating with no precession. An earth-horizon sensor is mounted γ degrees off the spacecraft z-axis so as to sweep over a cone which cuts the earth horizons at A and C. The inclination δ of the momentum vector to the subsatellite zenith vector may be expressed in terms of spacecraft elevation γ and horizon-pulse spacing. To summarize, we have just proved that

$$\cos\delta = \frac{-d\epsilon \pm f\sqrt{\epsilon^2 + f^2 - d^2}}{\epsilon^2 + f^2}, \quad \text{if } 0 \leqslant \delta \leqslant 180^\circ, \tag{D-13}$$

where

$d = \cos\rho$,

$\epsilon = \cos\gamma$,

and

$f = \sin\gamma \cos(\pi\Delta t_a/T_E)$.

Also, from Figures D-1 and D-2,

$\rho = \sin^{-1}[r_E/(r_E + h)]$,

Δt_a = horizon pulse spacing,

and

T_E = rotation period.

Information giving the value of δ is also contained in the relative position of the horizon pulses to the command-slit crossing of the sun. On the spacecraft, the earth horizon sensor has a pencil field of view located γ degrees from the spacecraft z-axis in the plane of the command slit. If the spacecraft is spinning so that $\theta = 0$, horizon pulses will be symmetrical about the instant when this plane crosses the center of the earth (see Figure D-3). The center of the earth is located on the celestial sphere at $(RA_z + 180^\circ)$ and $(-D_z)$ (see Figure 12), where RA_z is the right ascension and D_z is the declination of the subsatellite point zenith vector. The great-circle arc from the sun to the earth's center on the celestial sphere is $180^\circ - \eta$. The time midway between horizon pulses minus the time the command slit crosses the sun is Δt_c. The relationship between δ and Δt_c can now be written from the spherical triangles in Figure D-3.

The angle between $180^\circ - \delta$ and β is $\angle 2$, i.e., $(\dot\phi + \dot\psi)\Delta t_c$, as is used in Equation D-14, below. Since $\dot\phi + \dot\psi = \omega_z = 2\pi/T$, this angle can be expressed as $2\pi\Delta t_c/T$; this is how it appears in Figure D-3.

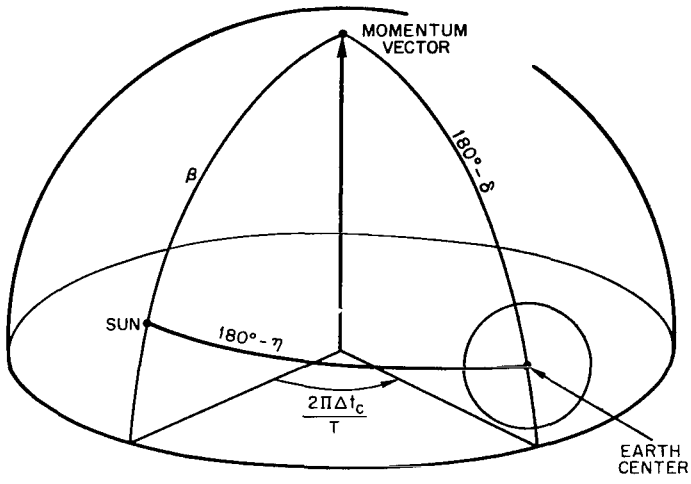

Figure D-3—Relationship between Δt_c and δ.

Thus, we have

$$\cos(180^\circ - \eta) = \cos\beta \cos(180^\circ - \delta) + \sin\beta \sin(180^\circ - \delta) \cos[(\dot{\phi} + \dot{\psi})\Delta t_c]\,; \qquad \text{(D-14)}$$

therefore,

$$\cos\eta = \cos\beta \cos\delta - \sin\beta \sin\delta \cos[(\dot{\phi} + \dot{\psi})\Delta t_c]\,. \qquad \text{(D-15)}$$

Solving for δ gives

$$\cos\delta = \frac{rs \pm \mu\sqrt{s^2 + \mu^2 - r^2}}{s^2 + \mu^2} \quad (0 \leqslant \delta \leqslant \pi)\,, \qquad \text{(D-16)}$$

where

$r = -\cos\eta$,

$s = -\cos\beta$,

and

$\mu = \sin\beta \cos[(\dot{\phi} + \dot{\psi})\Delta t_c]$.

Also, from Figure A-3,

$$\cos\eta = \sin D_z \sin D_s + \cos D_z \cos D_s \cos(RA_s - RA_z), \text{ if } 0 \leqslant \eta \leqslant 180^\circ, \qquad \text{(D-17)}$$

where

D_z = declination of subsatellite zenith,

D_s = declination of sun,

RA_z = right ascension of subsatellite zenith,

and

RA_s = right ascension of sun.

Appendix E

SCHEMATIC DIAGRAMS FOR ASPECT SYSTEM

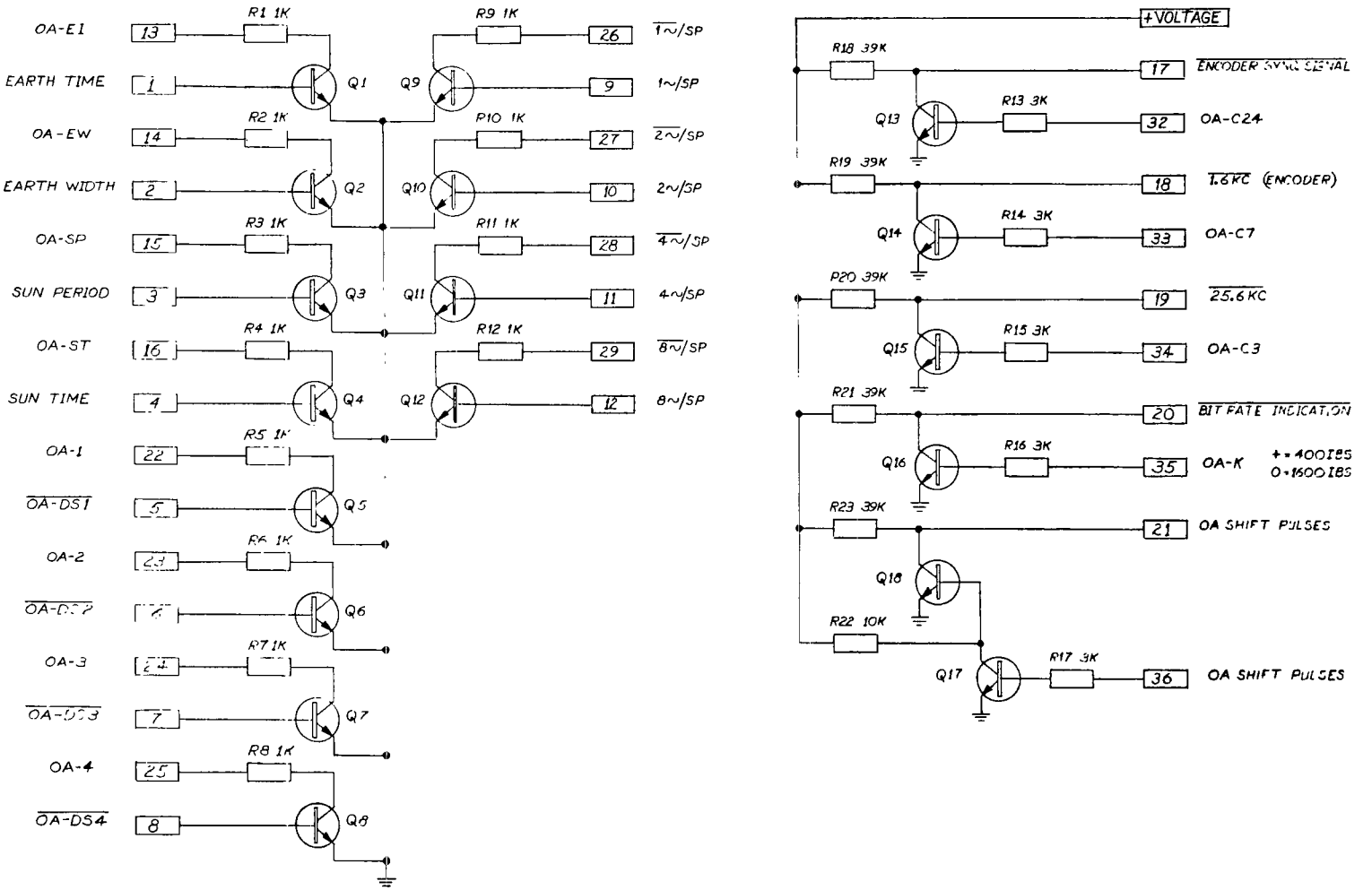

Figure E-1—IMP optical aspect: encoder interface module 16-176.

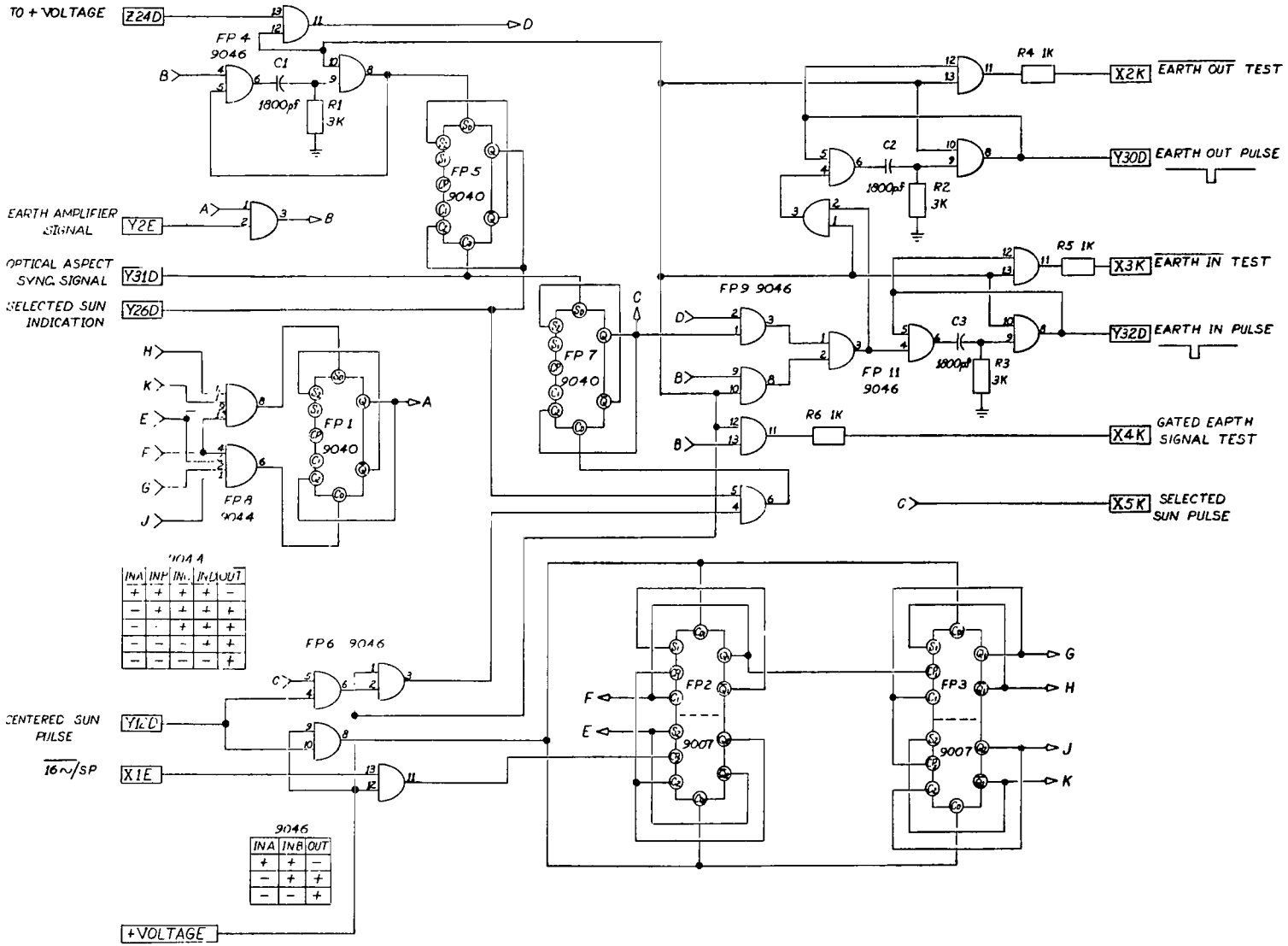

Figure E-2—IMP optical aspect: aspect module A 16-183.

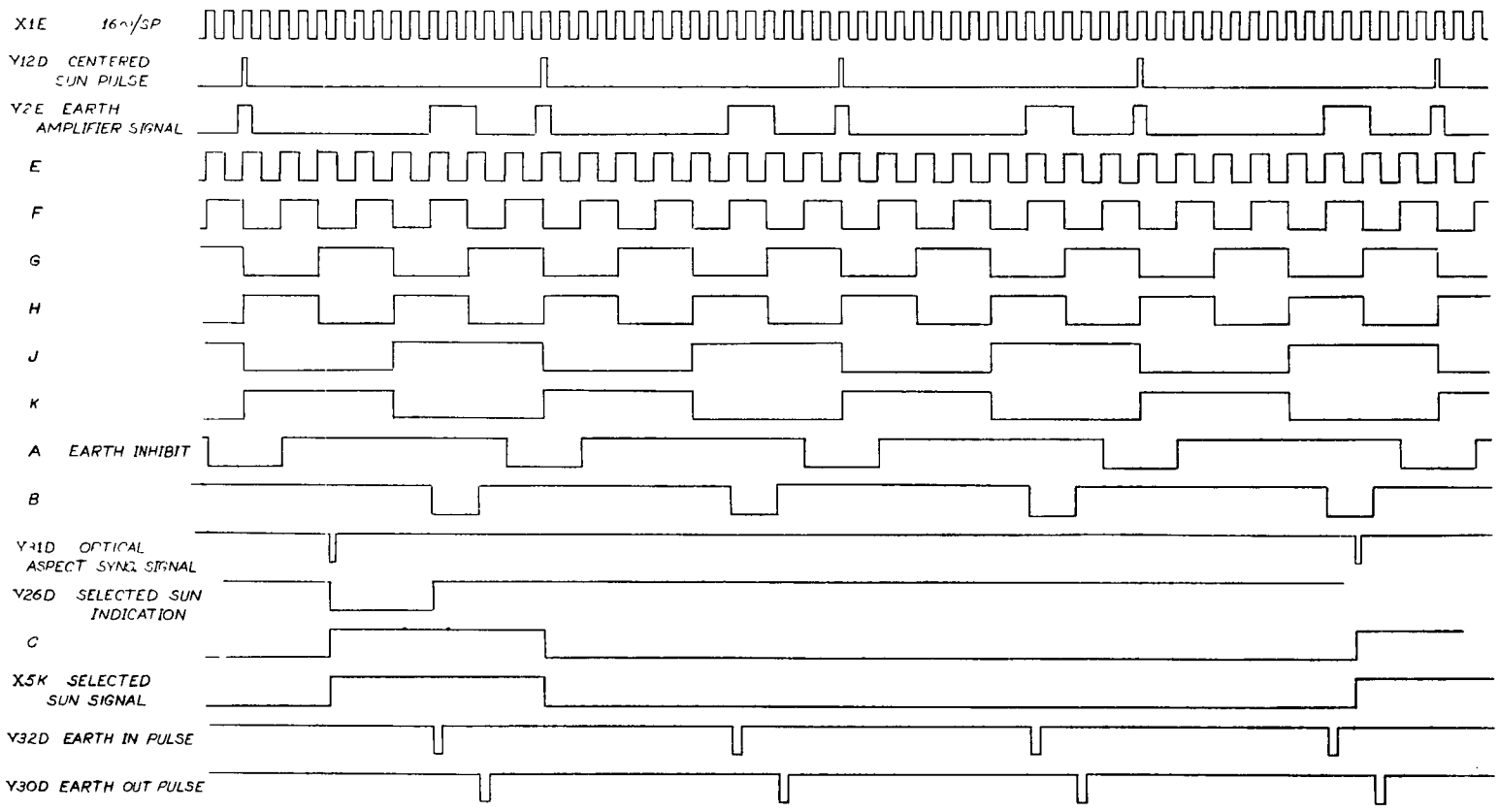

Figure E-3—IMP optical aspect: timing 16-183.

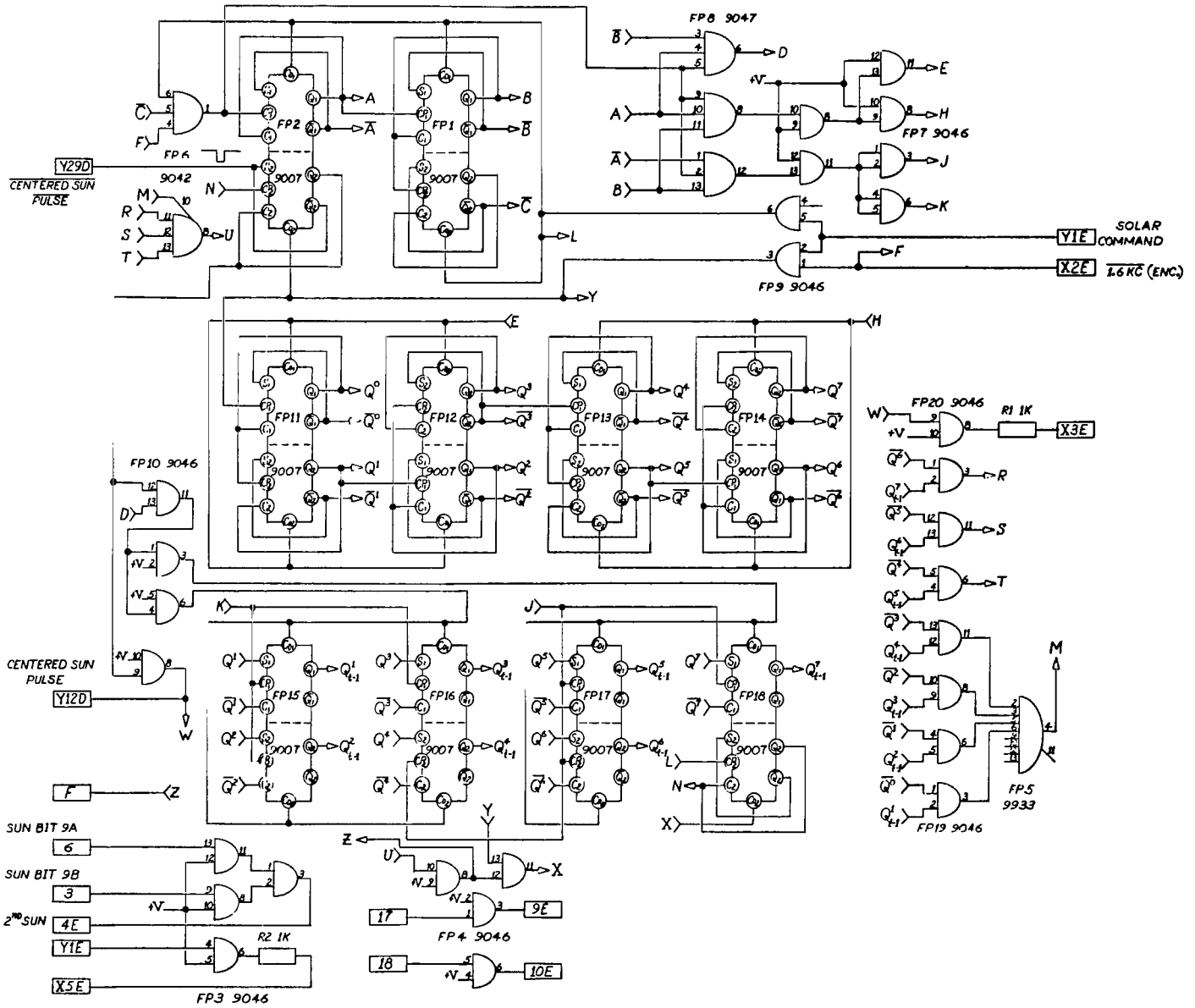

Figure E-4—IMP optical aspect: sun centering module 16-185.

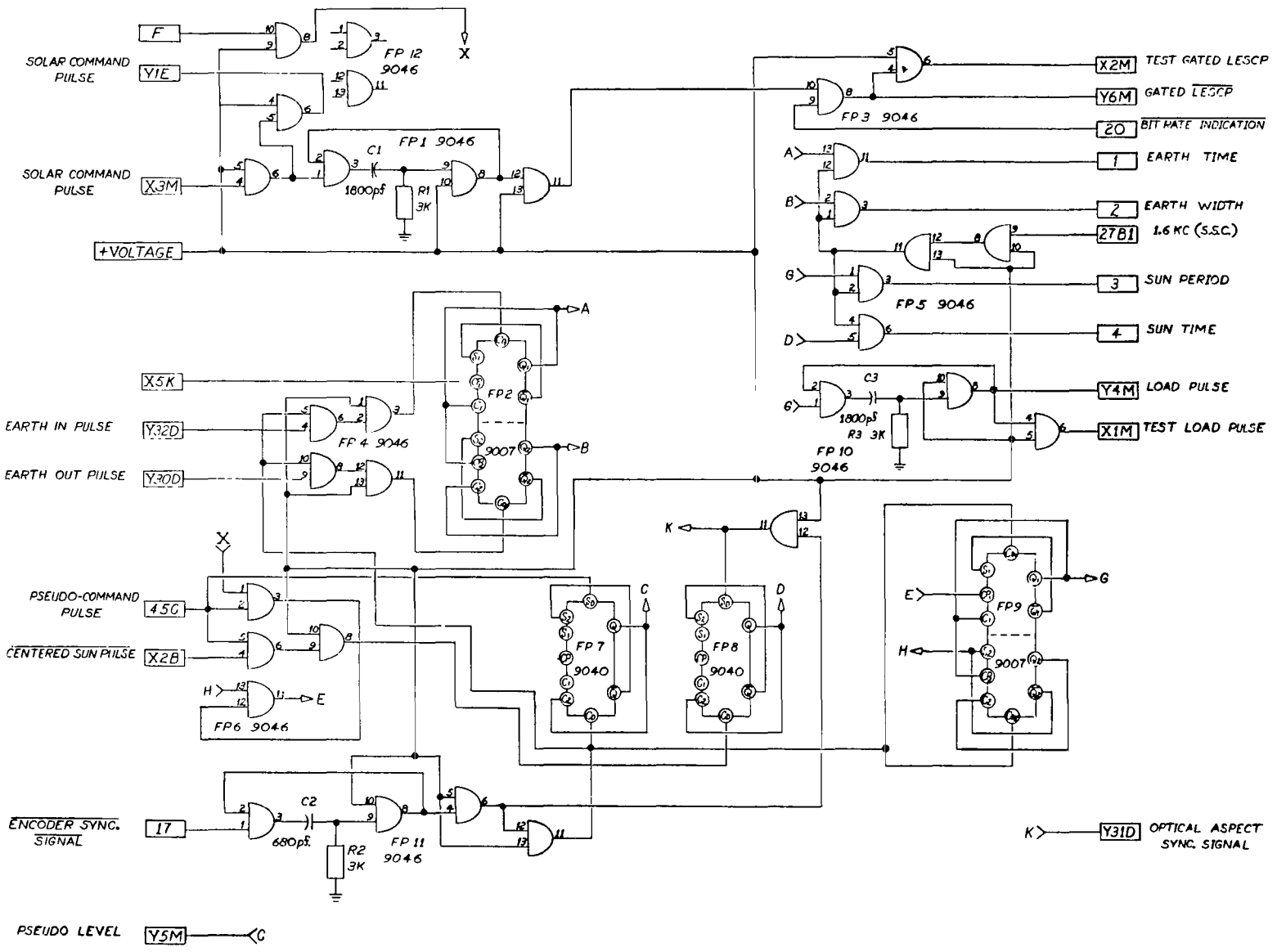

Figure F-5—IMP optical aspect: aspect module B 16-188.

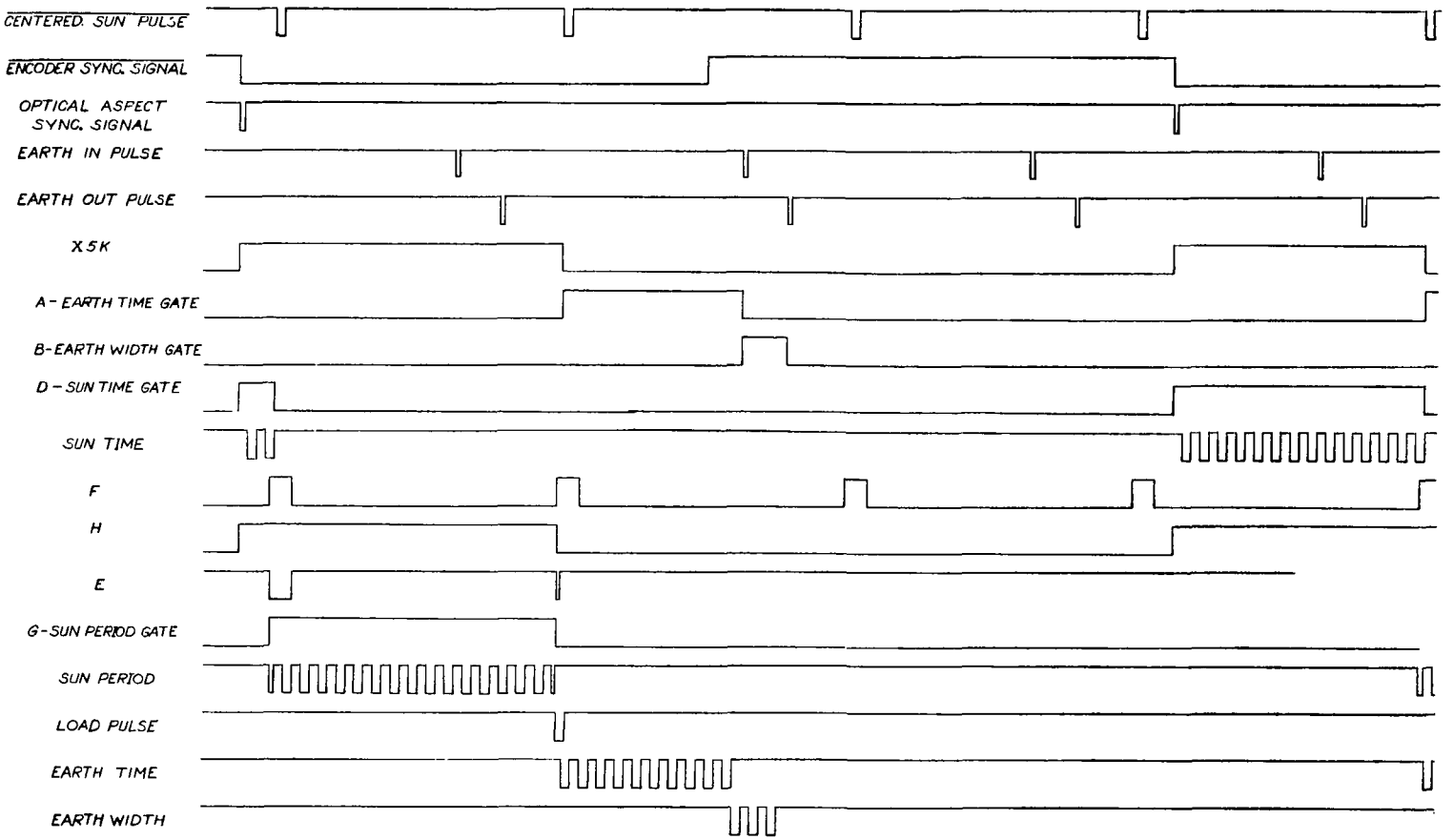

Figure E-6—IMP optical aspect: timing 16-188.

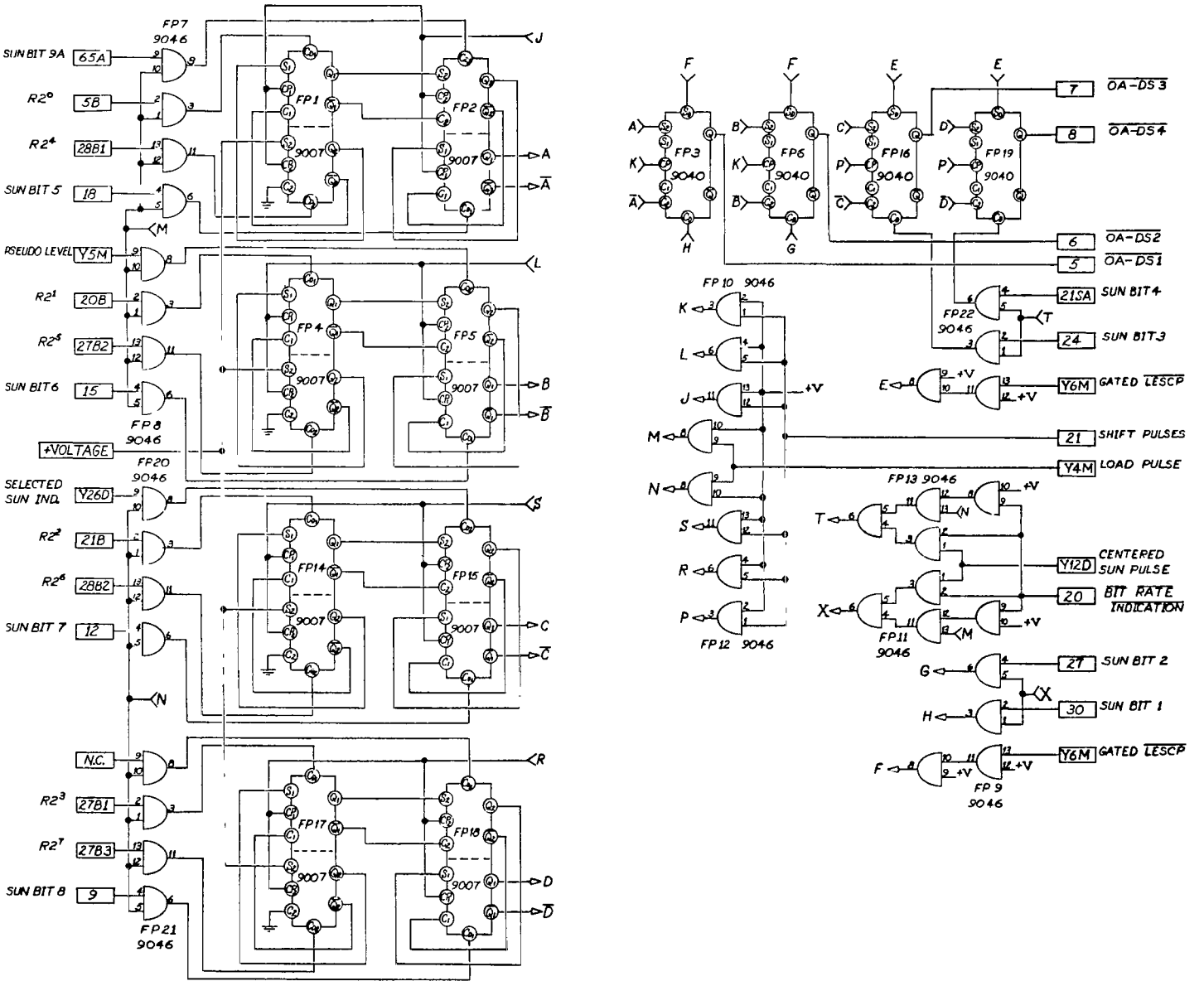

Figure E-7—IMP optical aspect: aspect module C 16-189.

Appendix F

SCHEMATIC DIAGRAMS FOR SSC SYSTEM

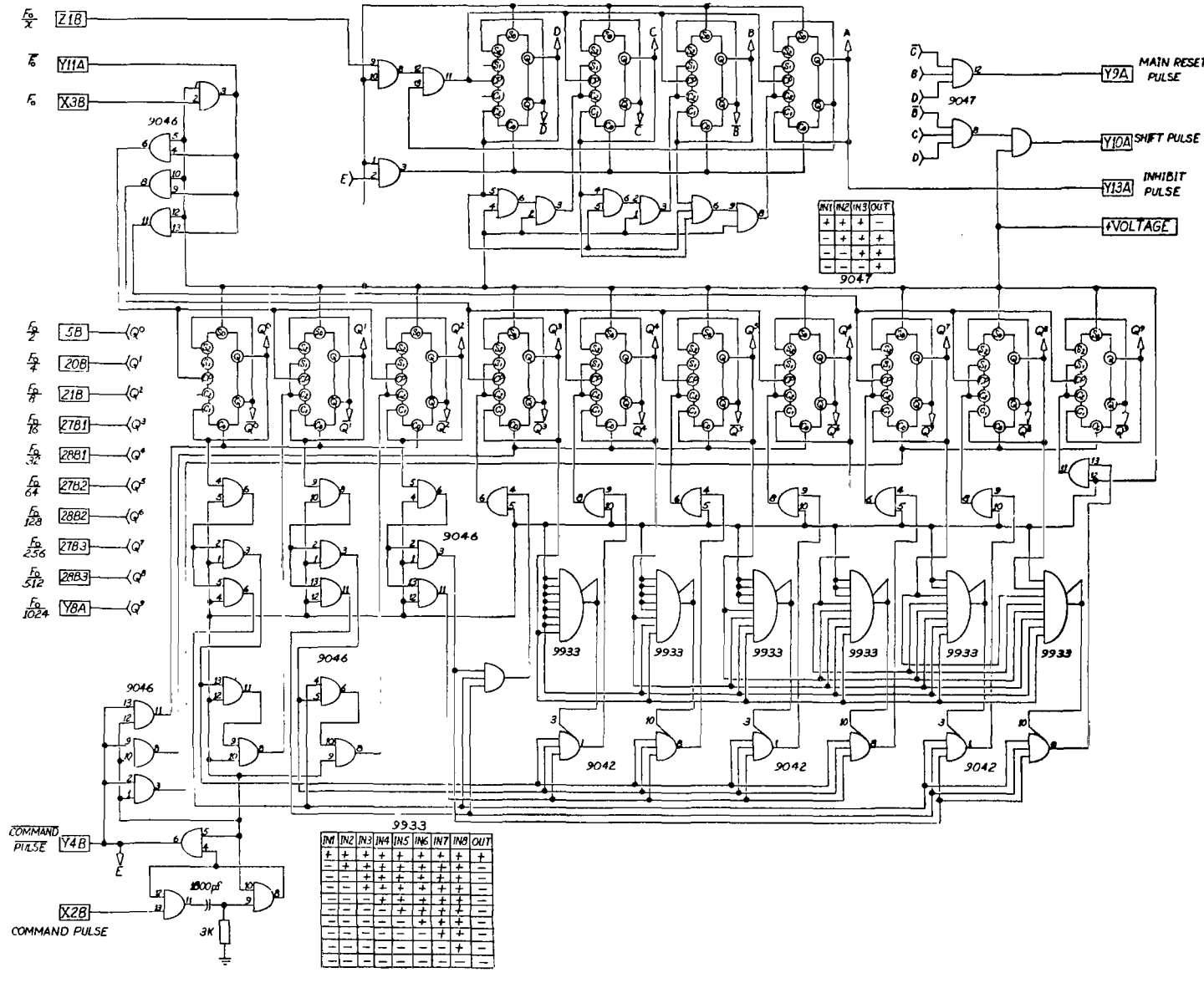

Figure F-1—IMP optical aspect: SSC function generator.

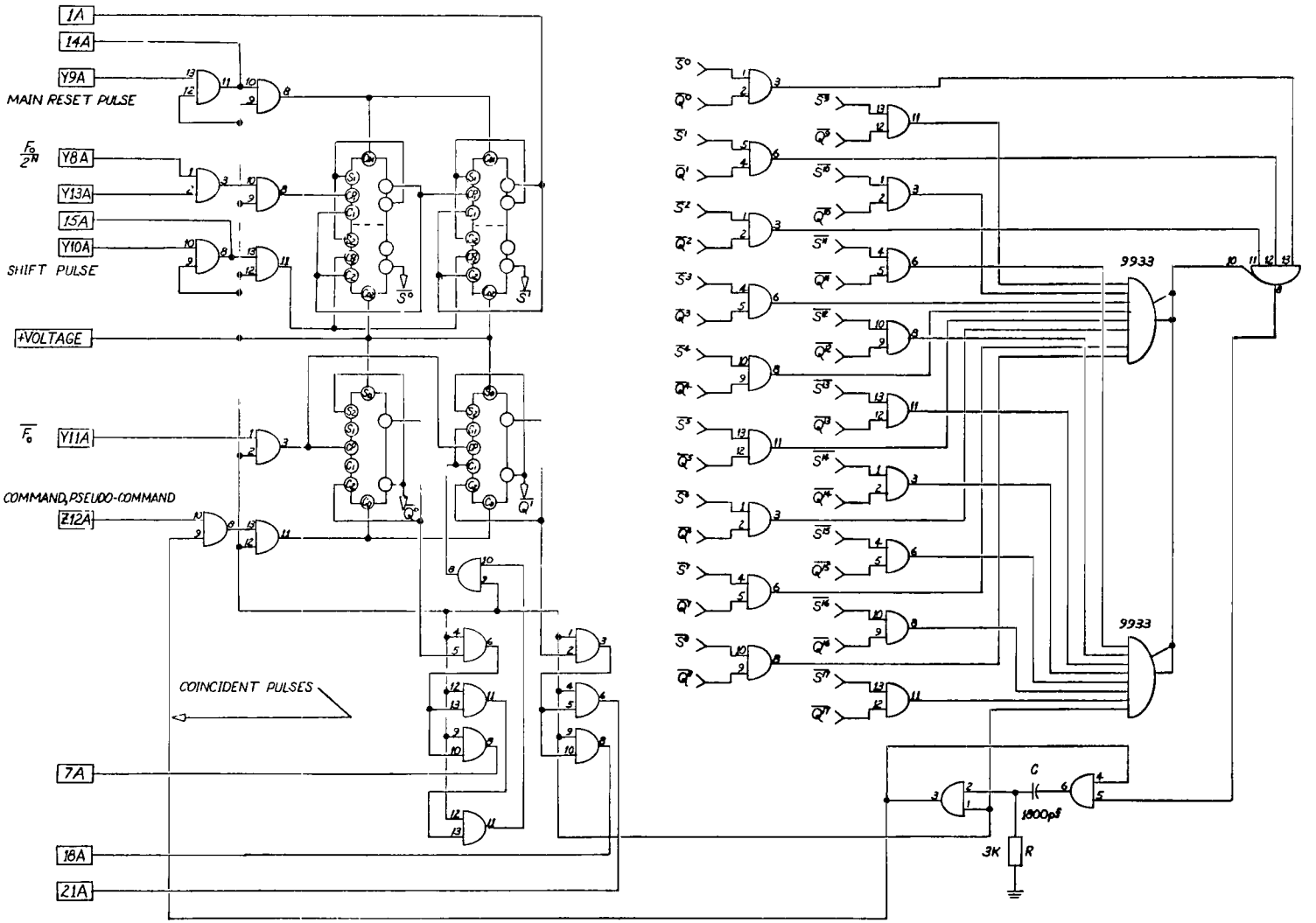

Figure F-2—IMP SSC, first section.

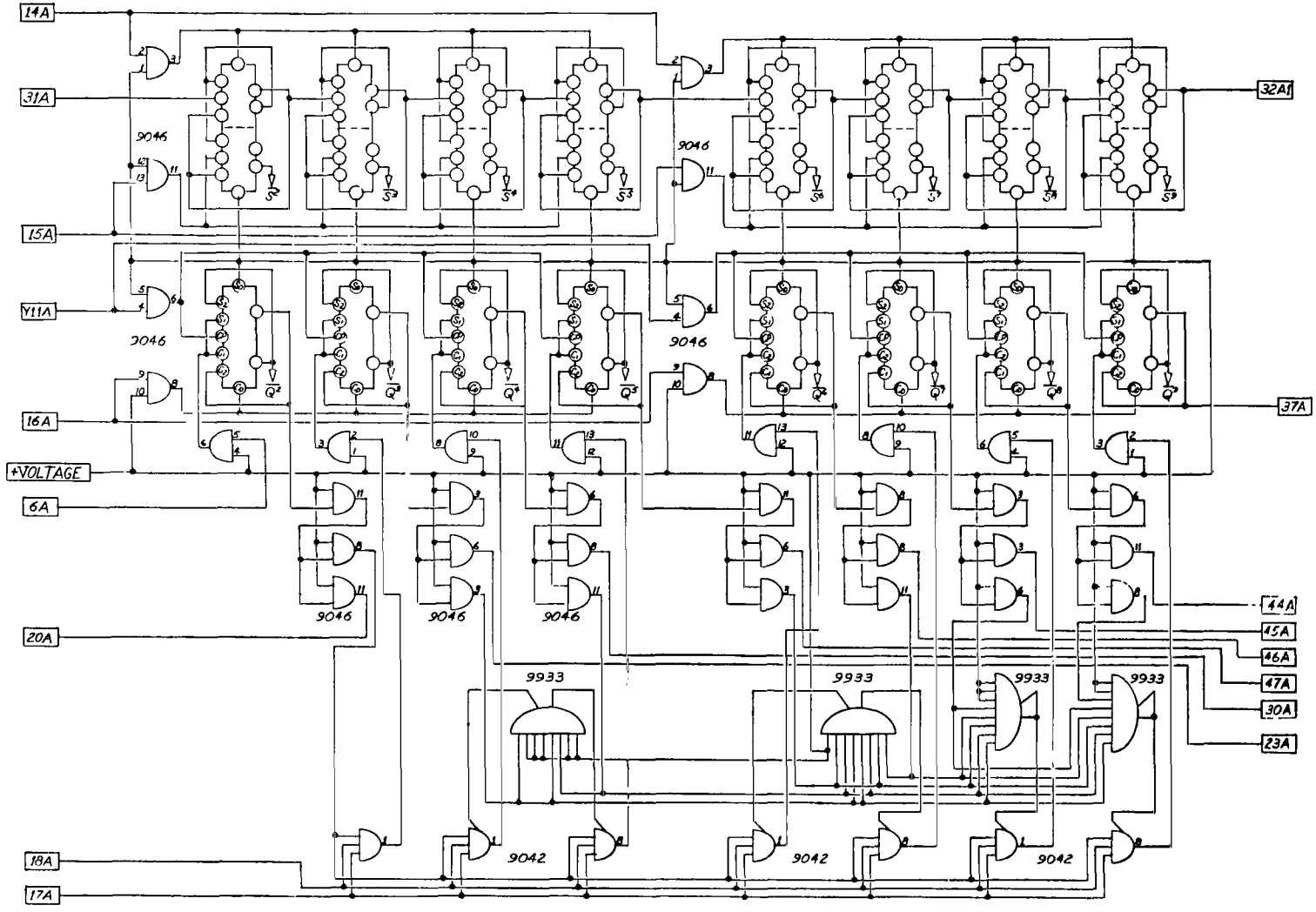

Figure F-3—IMP SSC, second section.

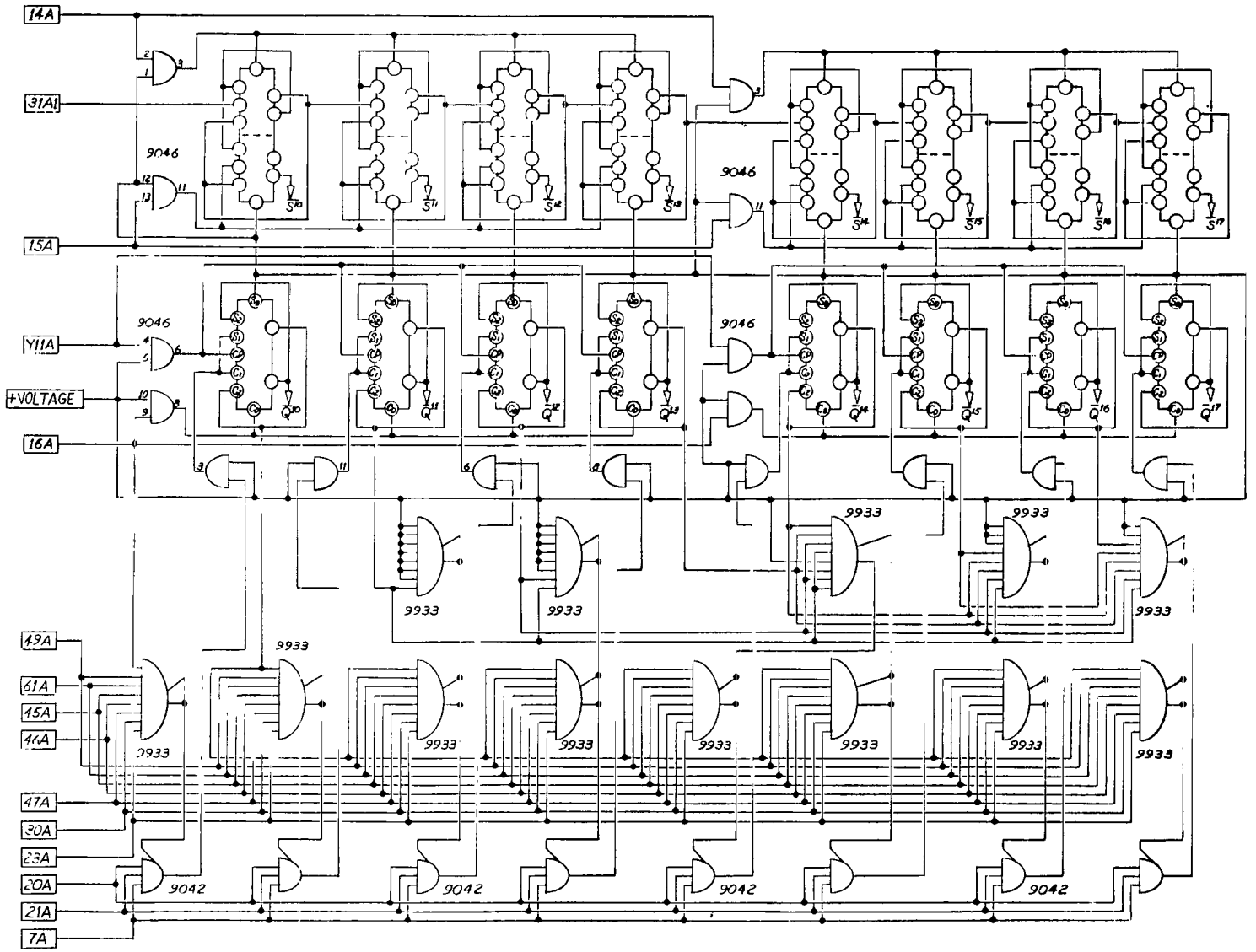

Figure F-4—IMP SSC, third section.

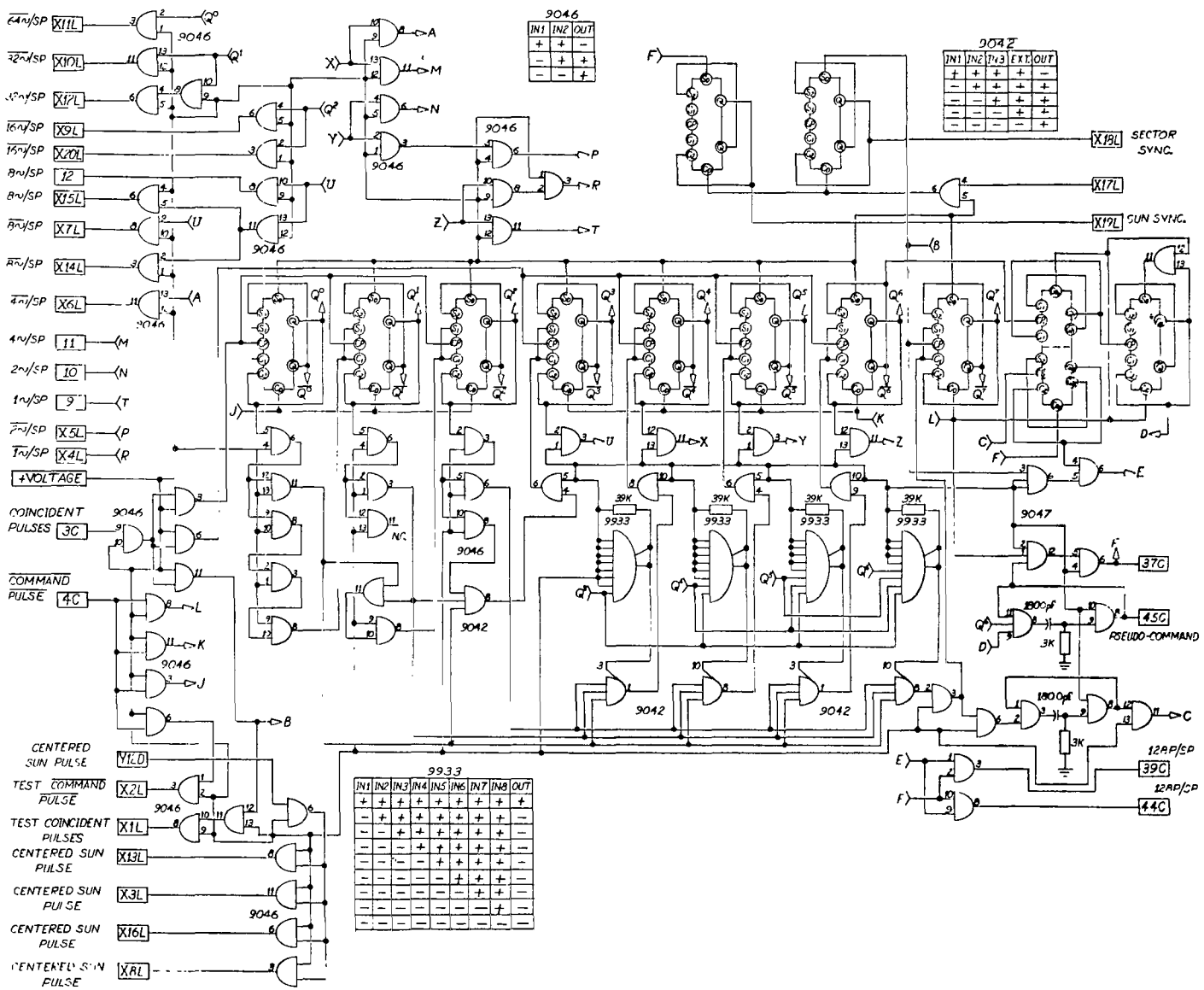

Figure F-5—IMP optical aspect: SSC output counter.

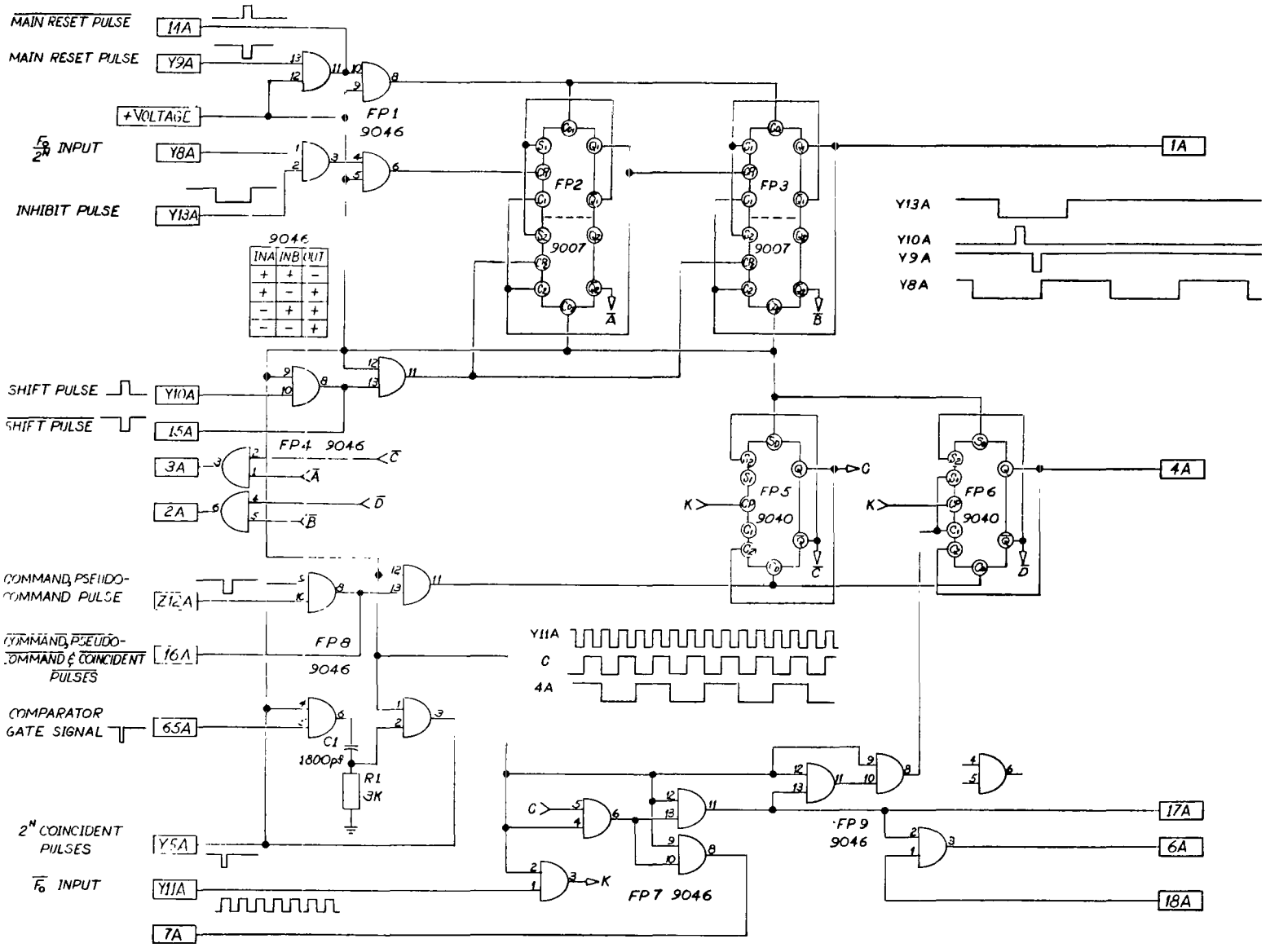

Figure F-6—IMP optical aspect: SSC 16-150.

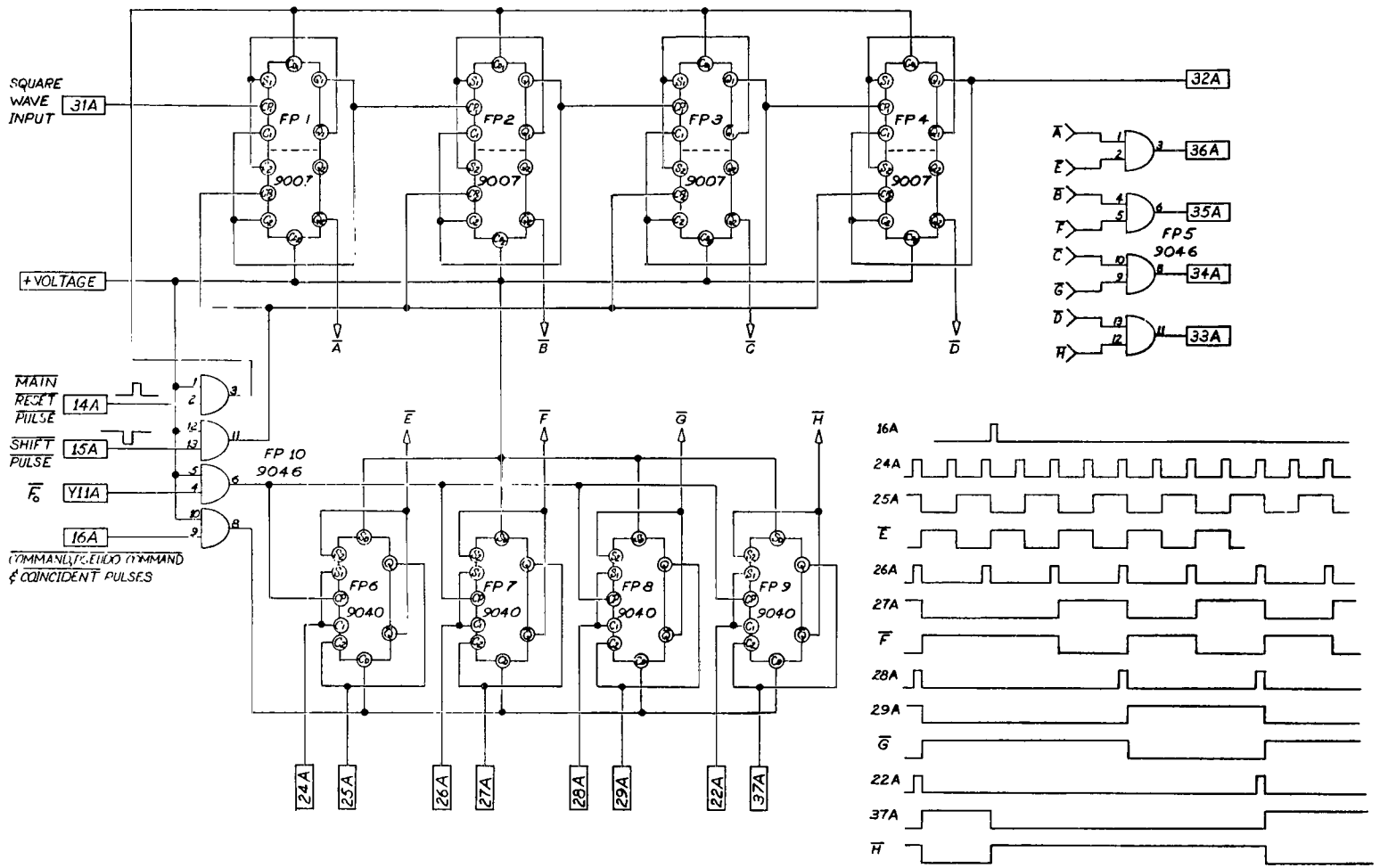

Figure F-7—IMP optical aspect: SSC 16-151.

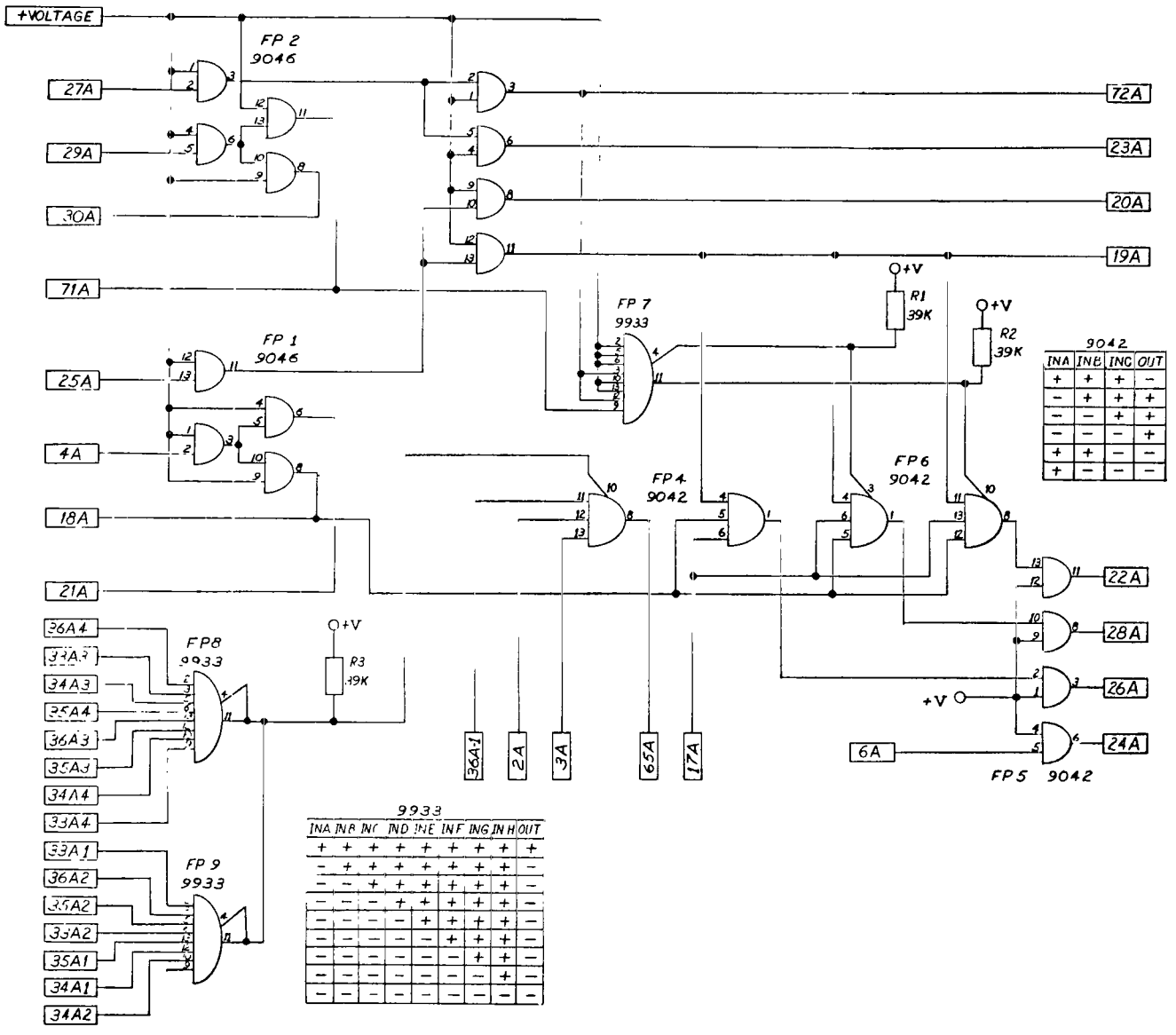

Figure F-8—IMP optical aspect: SSC 16-152.

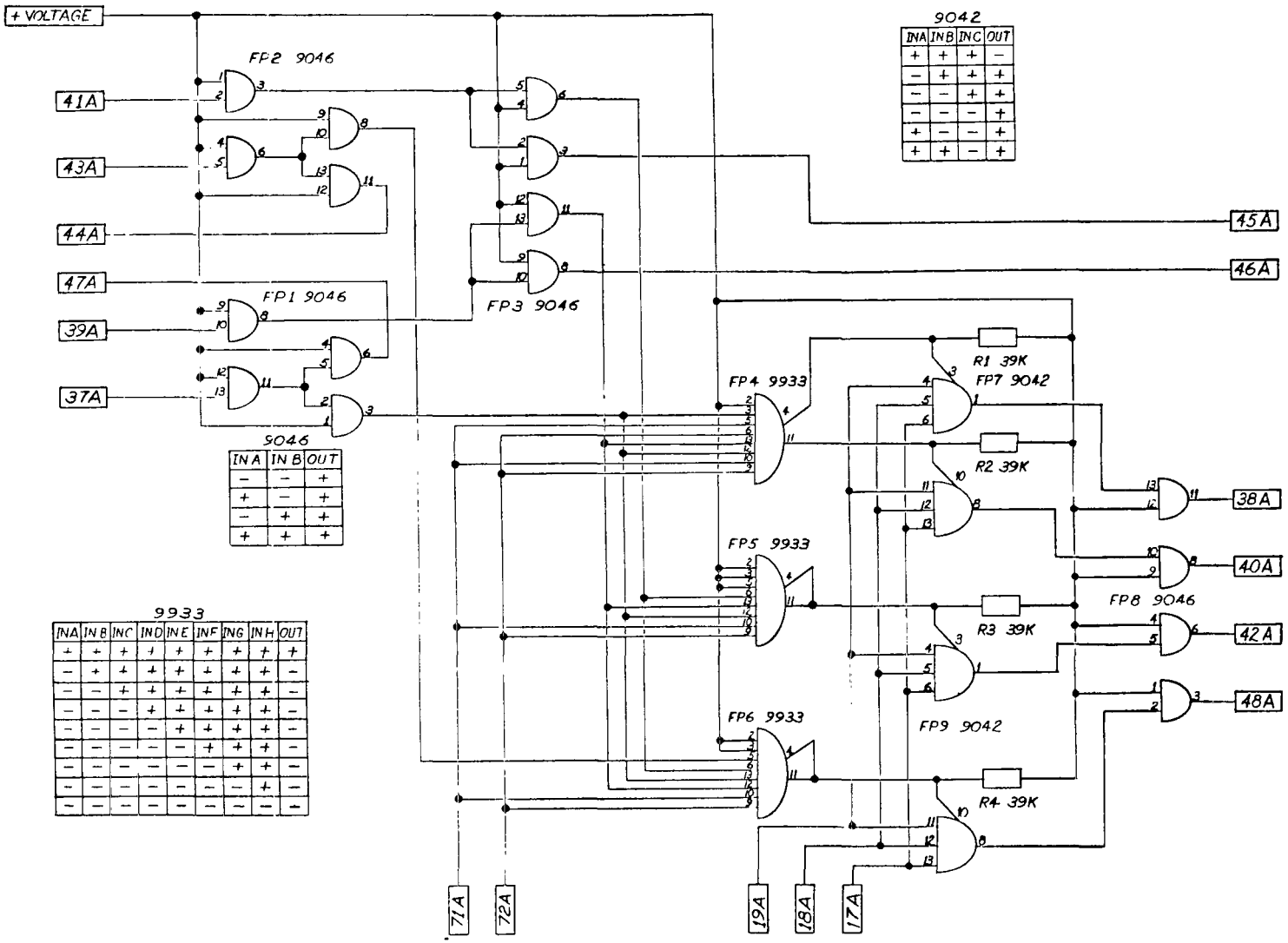

Figure F-9—IMP optical aspect: SSC 16-153.

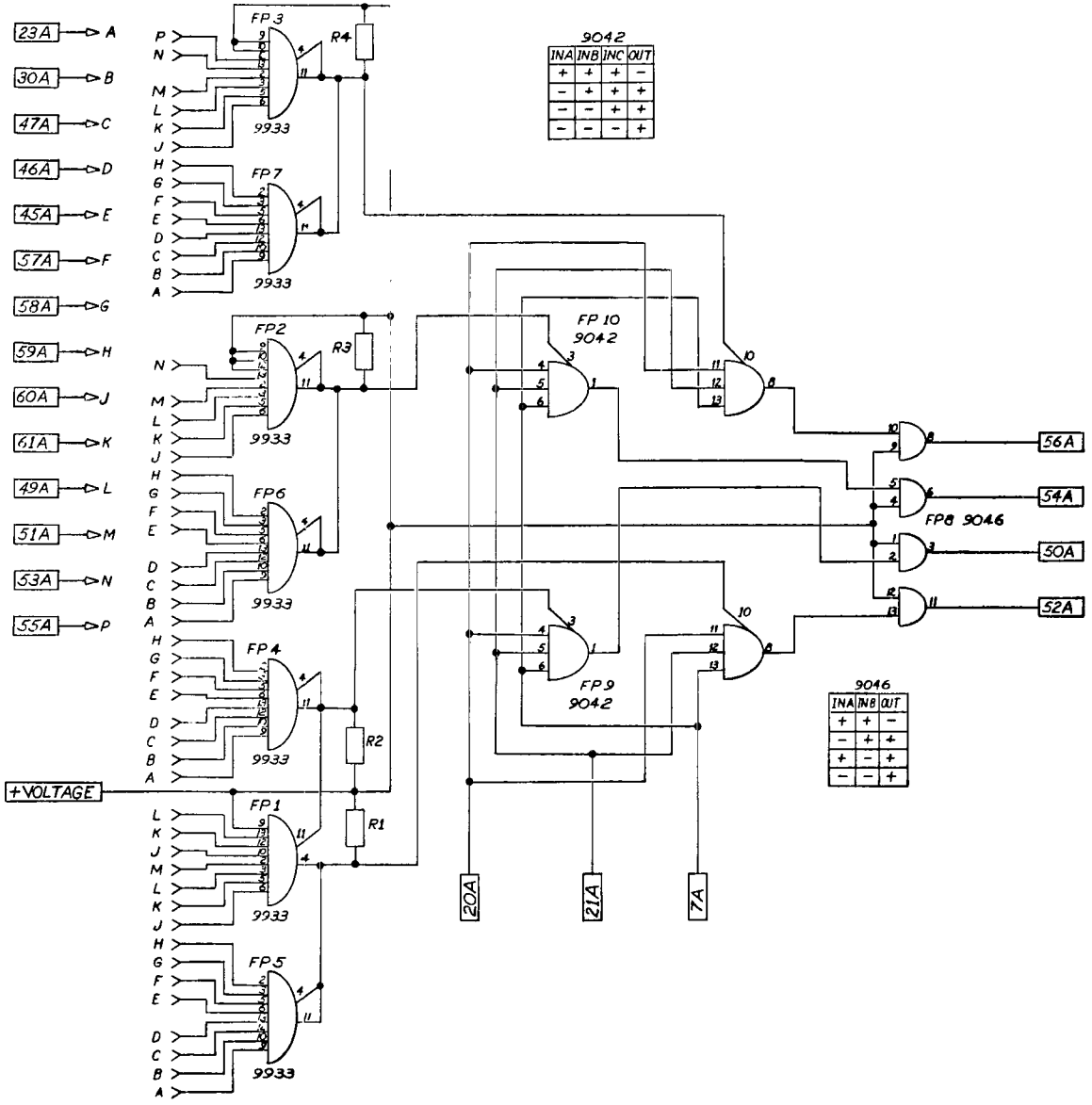

Figure F-10—IMP optical aspect: SSC 16-154.

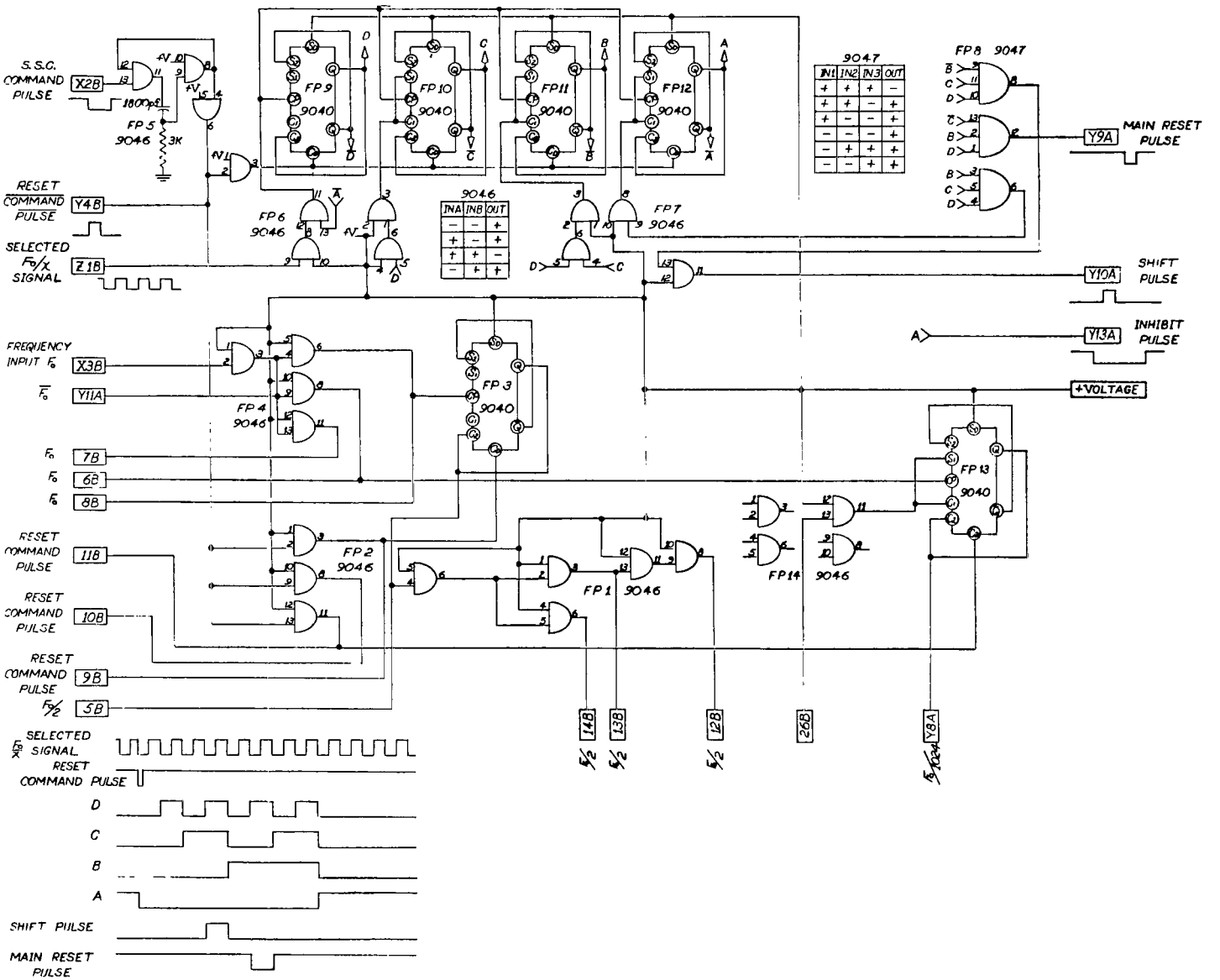

Figure F-11—IMP optical aspect: SSC 16-160.

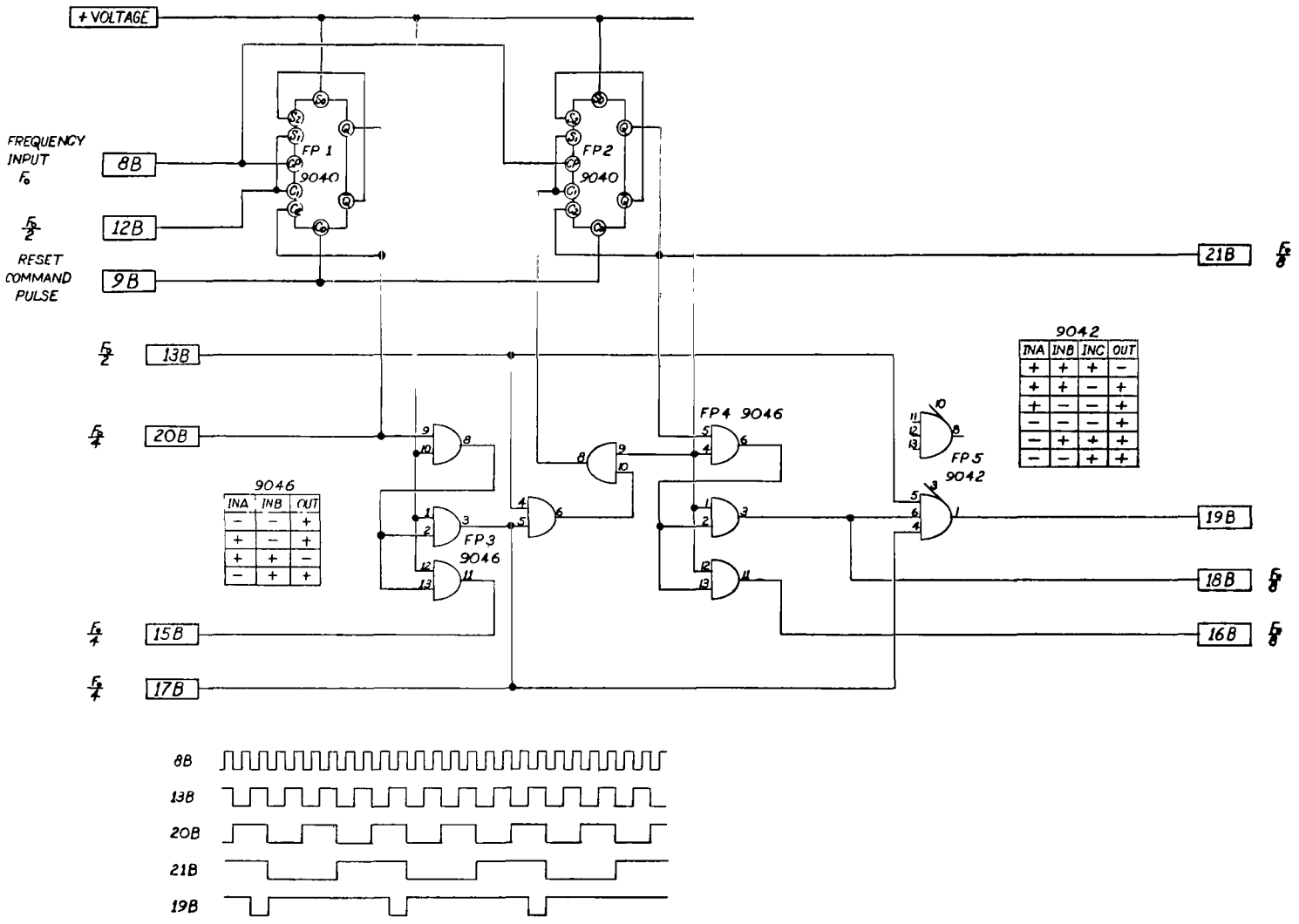

Figure F-12—IMP optical aspect: SSC 16-161.

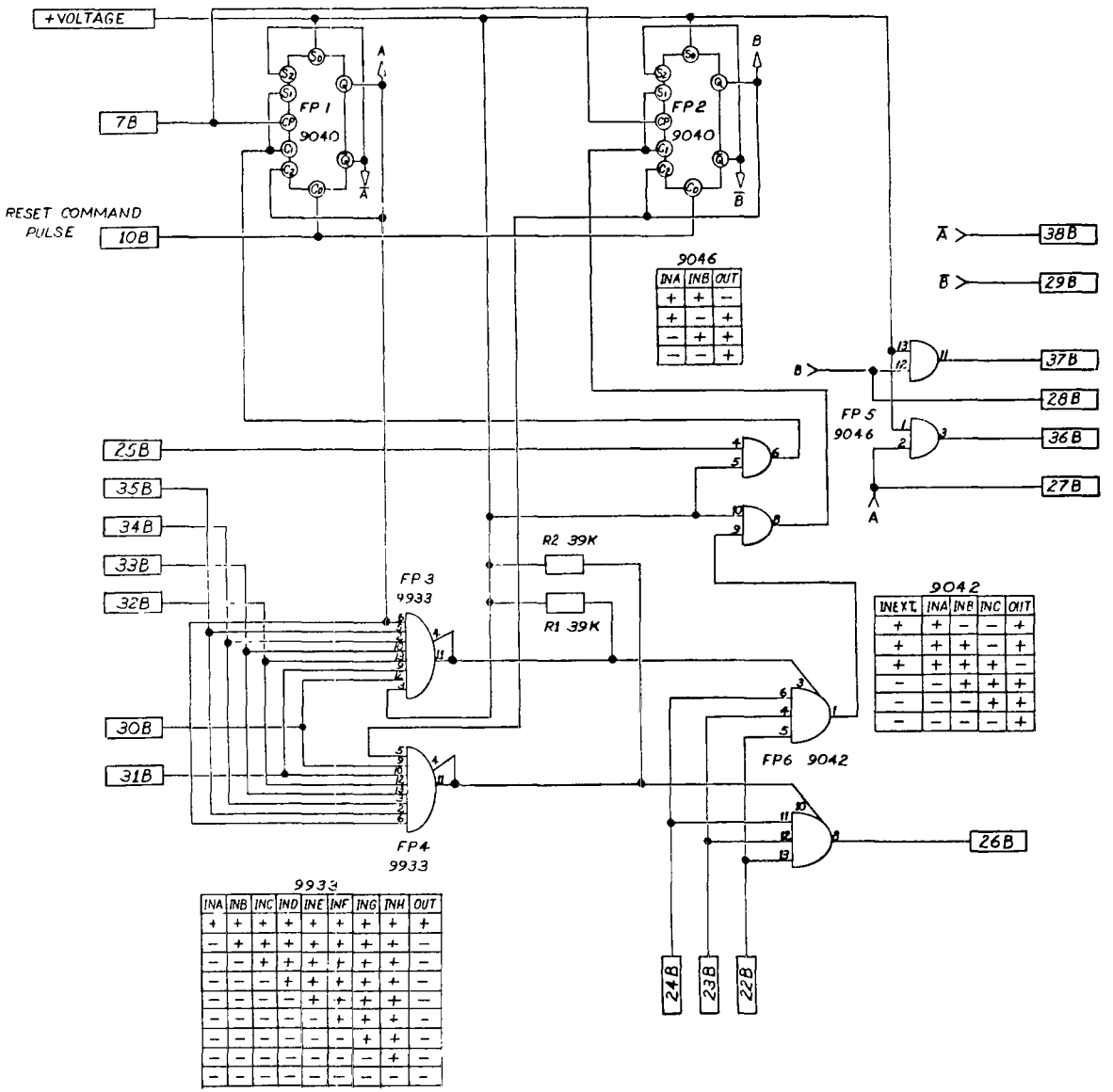

Figure F-13—IMP optical aspect: SSC 16-162

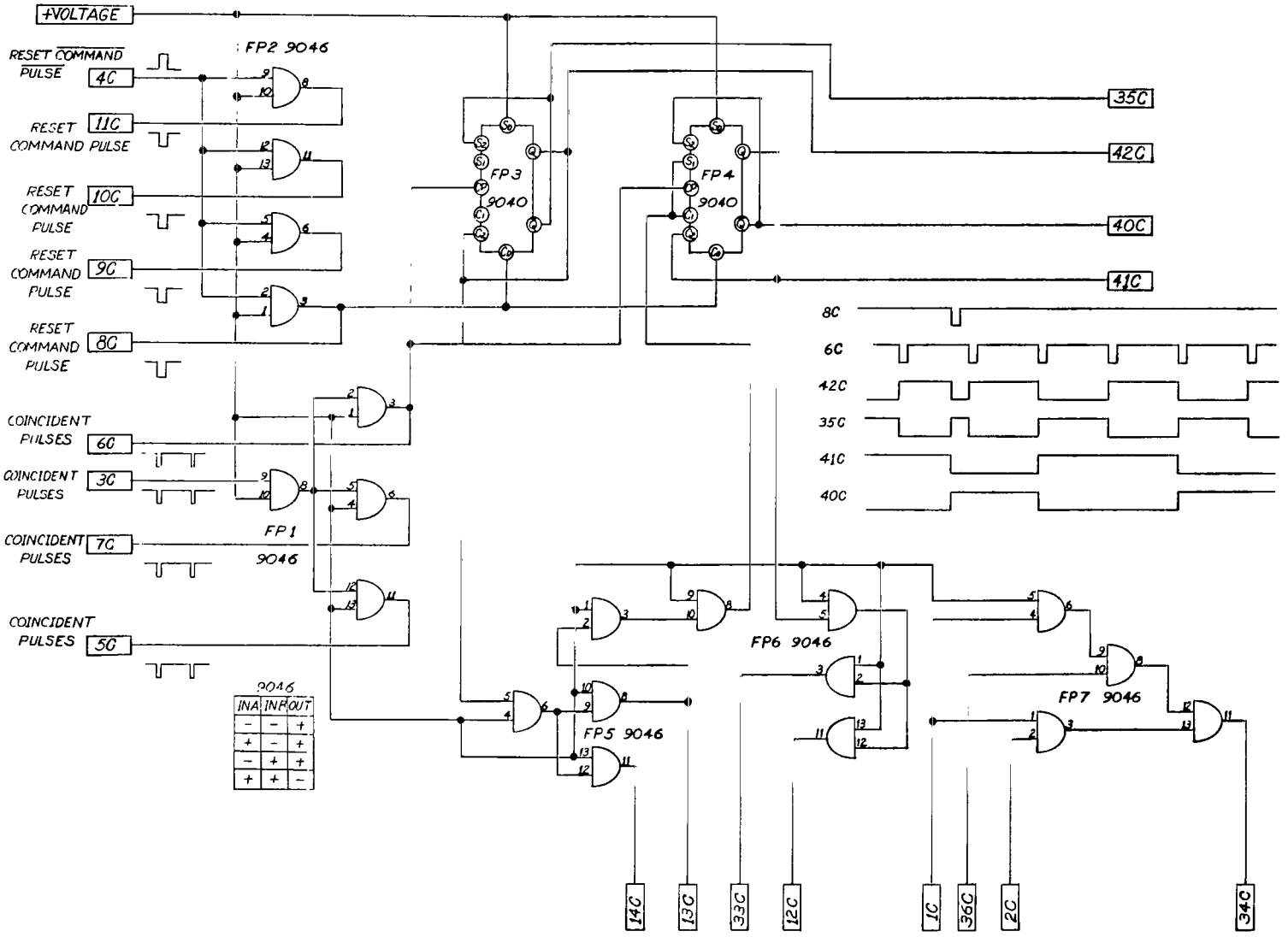

Figure F-14—IMP optical aspect: SSC 16-170.

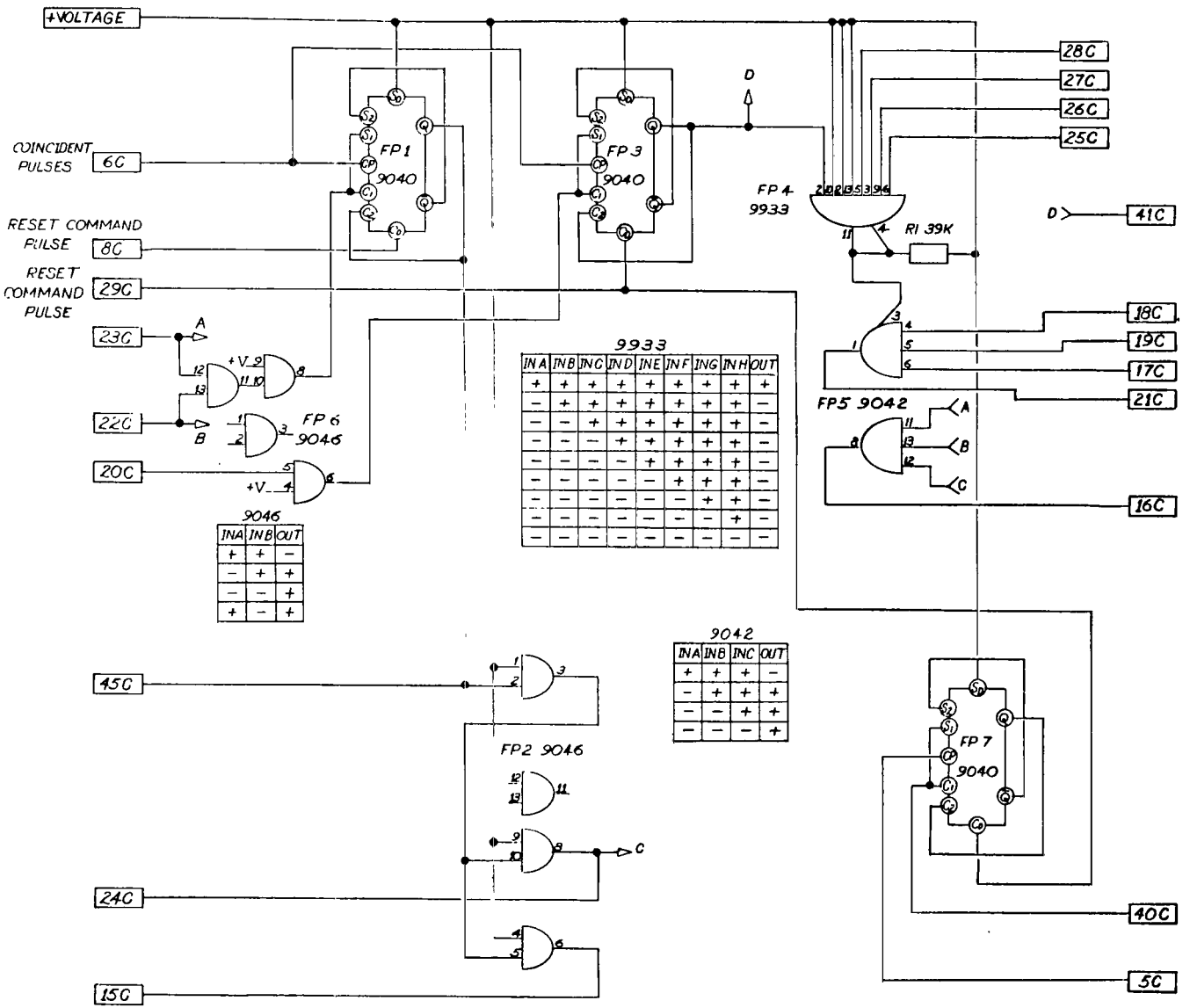

Figure F-15—IMP optical aspect: SSC 16-171.

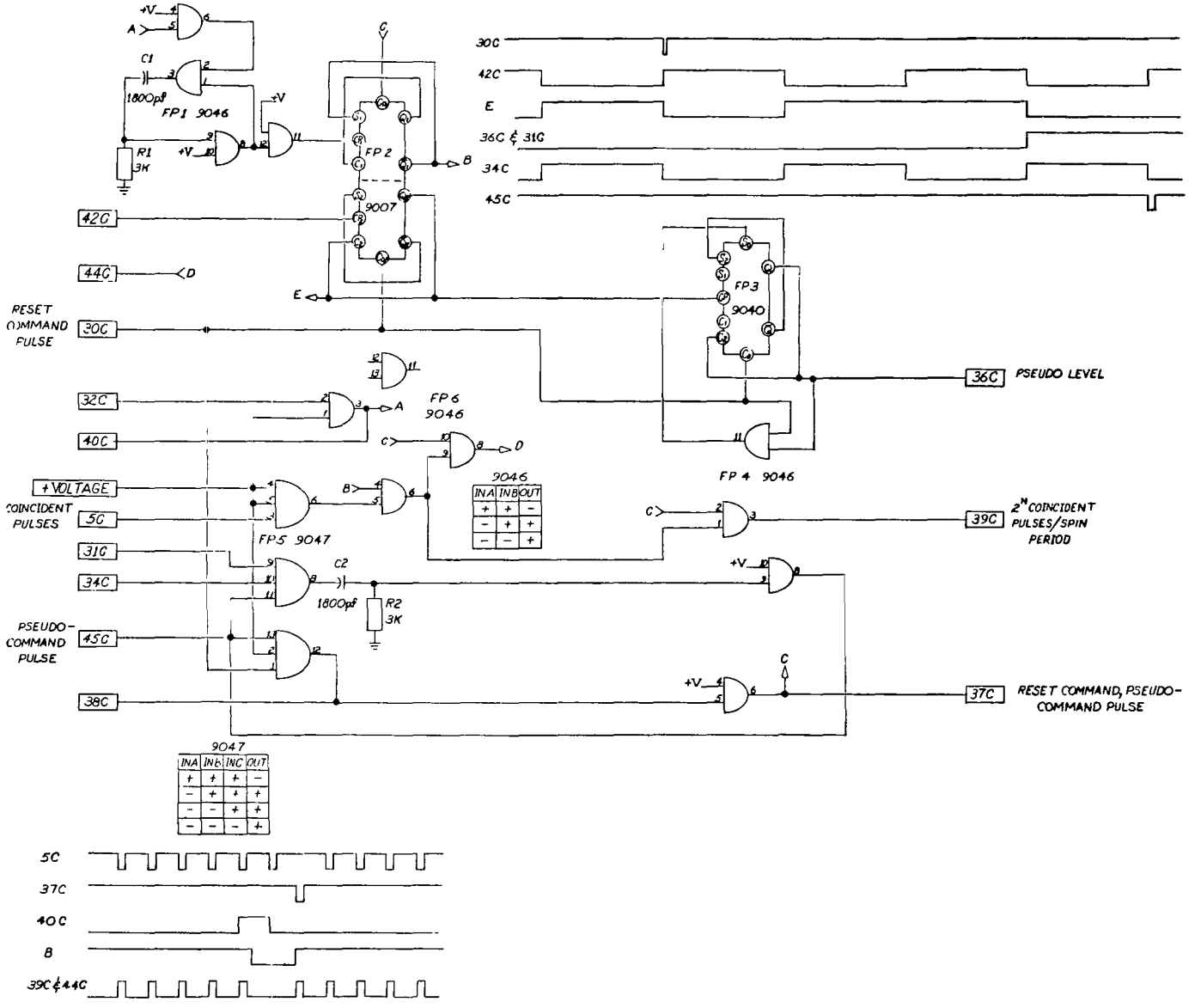

Figure F-16—IMP optical aspect: SSC 16-172.

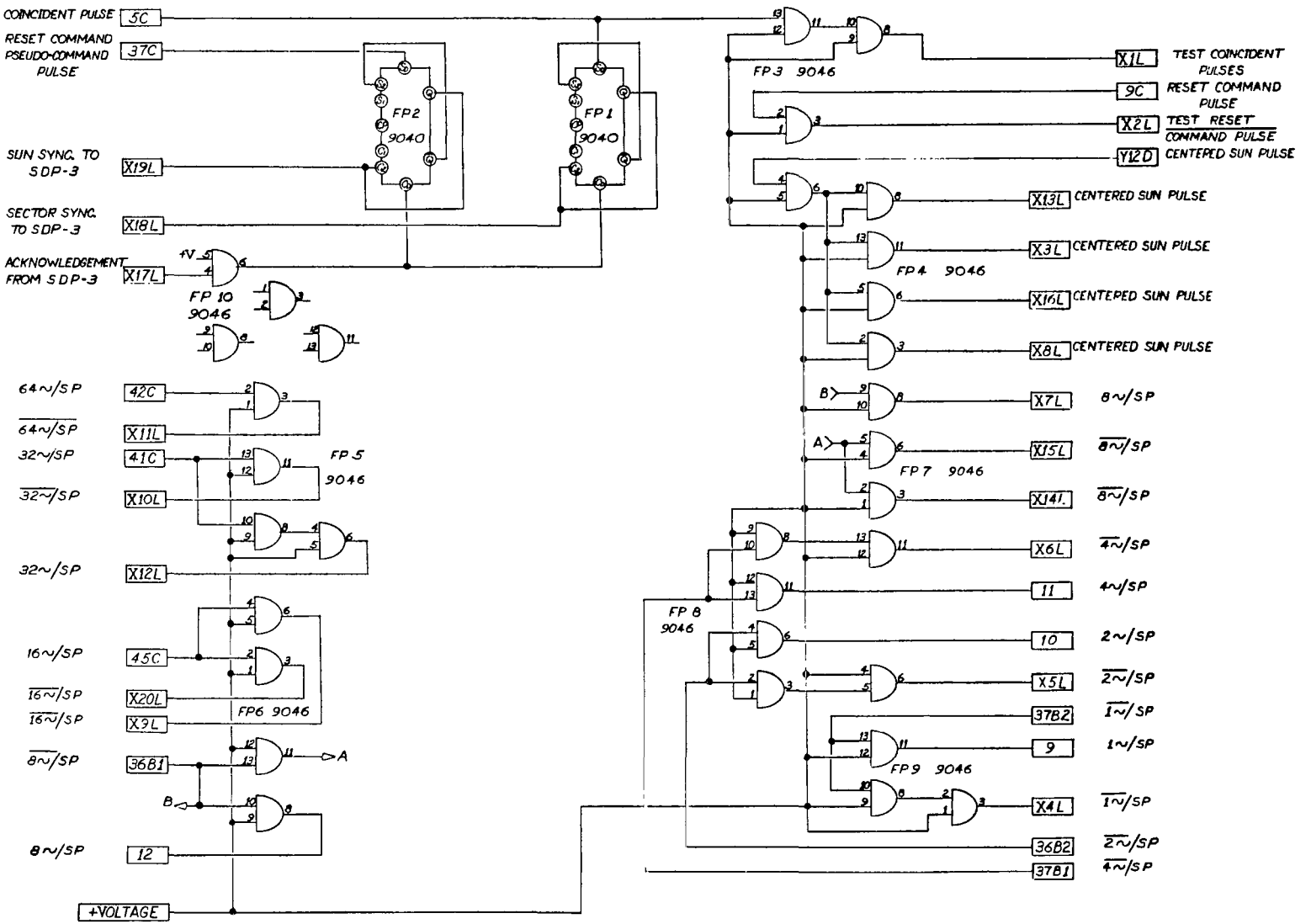

Figure F-17—IMP optical aspect: SSC 16-190.